Electronic Supporting Information (ESI) for

Roll-to-Roll Compatible Quinoxaline-Based Polymers toward High Performance Polymer Solar Cells

Mun Ho Yang,[a†] Seo-Jin Ko,[b†] Na Gyeong An,[c,d] Dong Ryeol Whang,[e] Seung-Hoon Lee,[b] Hyungju Ahn,[f] Jin Young Kim,[c] Doojin Vak,*[d] Sung Cheol Yoon,*[b] and Dong Wook Chang*[a]

[a]*Department of Industrial Chemistry, Pukyong National University,*

Busan, 48513 Republic of Korea

E-mail: dwchang@pknu.ac.kr

[b]*Division of Advanced Materials, Korea Research Institute of Chemical Technology (KRICT),*

Daejeon, 34114 Republic of Korea

E-mail: yoonsch@krict.re.kr

[c]*Department of Energy Engineering, Ulsan National Institute of Science and Technology*

(UNIST), Ulsan, 44919 Republic of Korea

[d]*CSIRO Manufacturing, Bag 10 Clayton South, Victoria, 3168 Australia*

E-mail: doojin.vak@csiro.au

[e]*Department of Advanced Materials, Hannam University, Daejeon, 34054 Republic of Korea.*

[f]*Industrial Technology Convergence Center, Pohang Accelerator Laboratory (PAL),*

Pohang, 37673 Republic of Korea.

[†]Mun Ho Yang and Seo-Jin Ko equally contributed to this research

1. Materials and Synthesis

1.1 Materials

2-buty-1-loctanol (**1**) were obtained from TCI. 5-fluoro-4,7-di(thiophen-2-yl)benzo[c][1,2,5]thiadiazole (**8**), (4,8-bis(5-(2-ethylhexyl)thiophene-2-yl)benzo[1,2-b:4,5-b']dithiophene-2,6-diyl)-bis(trimethylstannane) (**11**) and (4,8-bis(5-(2-ethylhexyl)-4-fluorothiophen-2-yl)benzo-[1,2-b:4,5-b']dithiophene-2,6-diyl)bis(trimethylstannane) (**12**) was synthesized according to the previous methods.[1-3] All other chemicals including lithium diisopropylamide (LDA), *N*-fluorobenzenesulfonmide (NFSI), tetrabutylammonium fluoride (TBAF), and *N*-bromosuccinimide (NBS) were purchased from Aldrich.

1.2 Synthesis

1.2.1. Synthesis of 5-(bromomethyl)undecane (2)

Triphenylphosphine (95.31mmol) was dissolved in dichloromethane (100 ml) under a N_2 atmosphere at 0°C. 2-Butyloctan-1-ol (**1,** 95.31 mmol) and bromine (6.79 ml, 133.44mmol) were carefully added into the solution, and the mixture was stirred at room temperature for overnight under N_2. Once the reaction was quenched by adding saturated aqueous solution of $NaHSO_3$, the mixture was poured into water and extracted with hexane. The organic layers were separated and dried over magnesium sulfate and filtered. Solvents were removed under reduced pressure, and the crude residue was purified by column chromatography with hexane. Yield: 93.6%. ^{1}H NMR (600 MHz, $CDCl_3$): δ (ppm) = 3.45 (d, *J* = 5.04 Hz, 2H), 1.60-1.57 (m, 1H), 1.39-1.20 (m, 16H), 0.91-0.87 (m, 6H). ^{13}C NMR (150 MHz, $CDCl_3$): δ (ppm) = 39.55, 39.27, 32.68, 32.36, 31.94, 29.60, 28.89, 26.65, 22.96, 22.77, 14.14, 14.10.

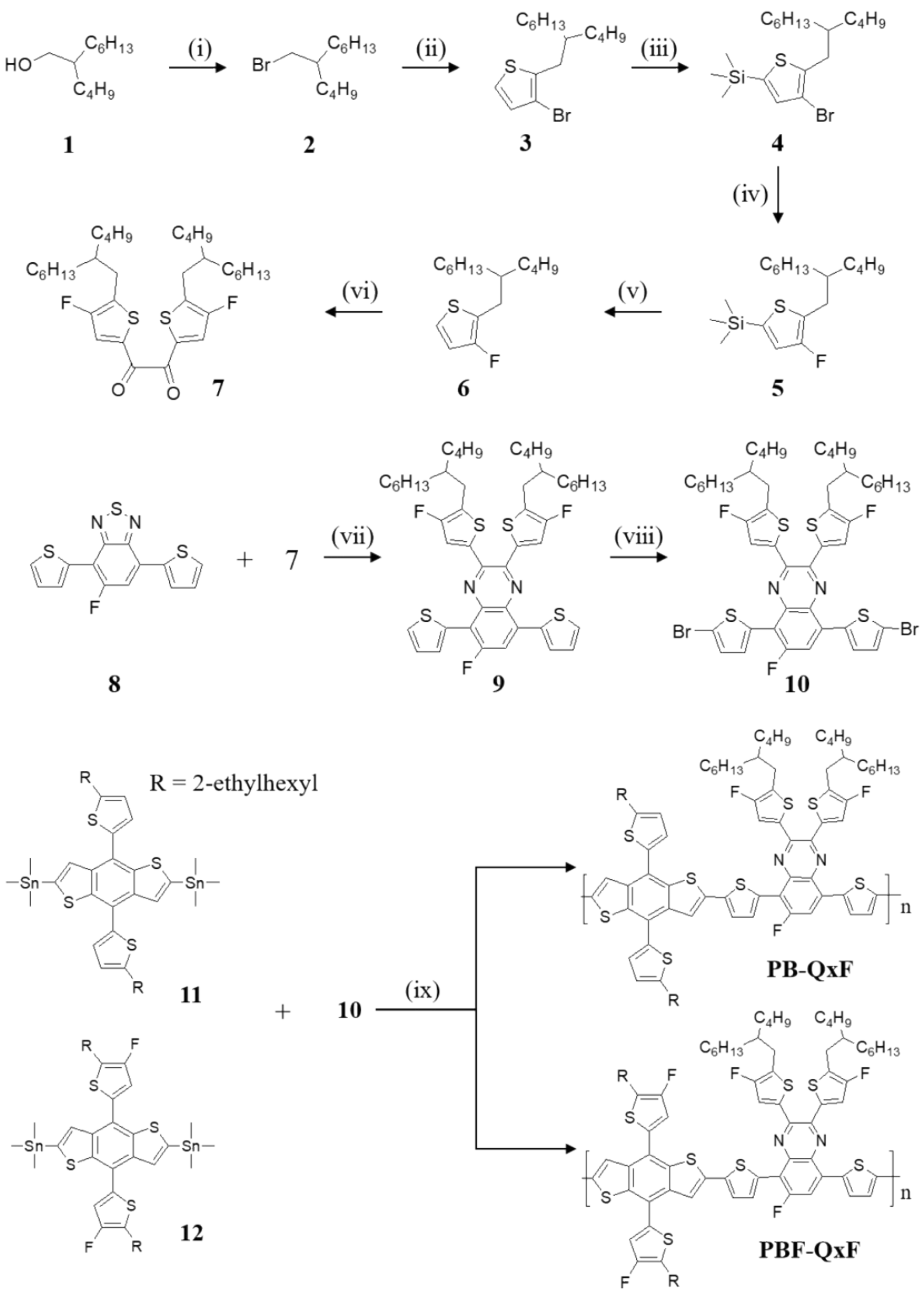

Scheme S1. Synthesis of monomers and polymers: (i) dichloromethane, P(Ph)$_3$, Br$_2$, overnight; (ii) LDA, THF, -78°C, overnight N$_2$; (iii) LDA, Me$_3$SiCl , THF, -78 °C, 5 h; (vi) NFSI, n-butyllithium, THF, -78 °C, 5 h; (v) TBAF, THF, RT, 3 h; (vi) n-butyllithium, CuBr, LiBr, oxalyl chloride, THF, -78 °C, 5 h; (vii) zinc, acetic acid, 80 °C, 4 h and then α-diketone, acetic acid, overnight; (viii) NBS, RT, overnight; (ix) Pd(PPh$_3$)$_4$, toluene, 80 °C, 48 h.

1.2.2. Synthesis of 3-bromo-2-(2-butyloctyl)thiophene (3)

After dissolving 3-bromothiophene (80 mmol) in dry THF (100 ml), LDA (96 mmol) was slowly added at - 78 °C under a N_2 atmosphere. The solution was stirred for 1 h and, subsequently, 5-(bromomethyl)undecane (80 mmol) was added. The mixture was additionally stirred for 1 h at - 78 °C and, thereafter, heated to reflux overnight. Once the reaction was completed, the mixture was poured into water and extracted with hexane. The organic layers were separated and dried over magnesium sulfate and filtered. Solvents were removed under reduced pressure, and the crude residue was purified by column chromatography with hexane. Yield: 60%. ^{1}H NMR (600 MHz, $CDCl_3$): δ (ppm) = 7.11 (d, *J* = 6Hz, 1H), 6.90 (d, *J*= 6Hz, 1H), 2.71 (d, *J* = 6Hz 2H), 1.7 (s, 1H) 1.30-1.26 (m, 16H), 0.90-0.86 (m, 6H). ^{13}C NMR (150 MHz, $CDCl_3$): δ (ppm) = 138.99, 129.83, 123.12, 109.44, 39.61, 33.75, 33.36, 33.06, 32.06, 29.82, 26.64, 23.19, 22.87, 14.29.

1.2.3. Synthesis of (4-bromo-5-(2-butyloctyl)thiophene-2-yl)trimethylsilane (4)

After dissolving **3** (30,01mmol) in dry THF (100 ml) under a N_2 atmosphere, LDA (54.02 mmol) was slowly added at -78°C under a N_2 atmosphere. After stirring for 1 h, Me_3SiCl (54.02 mmol) was added slowly, and subsequently stirred 6 h at room temperature. Once the reaction was completed, the mixture was poured into water and extracted with hexane. The organic layers were separated and dried over magnesium sulfate and filtered. Solvents were removed under reduced pressure, and the crude residue was purified by column chromatography with hexane. Yield: 78%. ^{1}H NMR (600 MHz, $CDCl_3$): δ (ppm) = 6.89 (s, 1H), 2.61 (d, *J*= 6Hz, 2H), 1.59 (s, 1H) 1.19-1.14 (m, 16H), 0.78-0.75 (m, 6H) 0.28 (d, *J* = 2Hz, 10H). ^{13}C NMR (150 MHz, $CDCl_3$): δ (ppm) = 144.23, 137.99, 136.22, 110.62, 39.52. 33.94, 33.32, 33.07, 32.70, 32.00, 29.73, 28.85, 26.56, 23.12, 22.80, 14.25, -0.15.

1.2.4. Synthesis of (5-(2-butyloctyl)-4-fluorothiophene-2-yl)trimethylsilane (5)

After dissolving **4** (24.78mmol) in dry THF (100ml) under a N_2 atmosphere, n-butyllithium (37.17mmol, 2.5M in hexane) was added slowly at -78 °C. After stirring for 1 h, the solution of NFSI (49.56 mmol) in dry THF (50 ml) was added, and subsequently, stirred for 5hr at room temperature. Once the reaction was completed, the mixture was poured into water and extracted with hexane. The organic layers were separated and dried over magnesium sulfate and filtered. Solvents were removed under reduced pressure, and the crude residue was purified by column chromatography with hexane. Yield: 60%. ^{1}H NMR (600 MHz, $CDCl_3$): δ (ppm) = 6.85 (s, 1H), 2.65 (d, *J*= 6Hz, 2H), 1.60 (s, 1H) 1.28-1.26 (m, 16H), 0.90-0.87 (m, 6H) 0.27 (d, *J* = 2Hz, 10H). ^{13}C NMR (150 MHz, $CDCl_3$): δ (ppm) = 155.44, 133.86, 123.39, 123.23, 39.44, 33.36, 33.08, 32.01, 29.78, 28.91, 26.61, 23.13, 22.81, 14.21, -0.33.

1.2.5. Synthesis of 2-(2-butyloctyl)-3-fluorothiophene (6)

After dissolving **5** (18.6 mmol) in dry THF (100 ml) under a N_2 atmosphere, TBAF (22.32 mmol, 1.0 M in THF) was added slowly at -78 °C. After stirring for 3 h at room temperature, the mixture was poured into water and extracted with hexane. The organic layers were separated and dried over magnesium sulfate and filtered. Solvents were removed under reduced pressure, and the crude residue was purified by column chromatography with hexane. Yield: 88%. ^{1}H NMR (600 MHz, $CDCl_3$): δ (ppm) = 6.96 (dd, *J* = 3.54, 5.52Hz, 1H), 6.72 (d, *J*= 5.52Hz, 1H), 2.65 (d, *J* = 6.54Hz 2H), 1.6 (s, 1H) 1.28-1.26 (m, 16H), 0.93-0.86 (m, 6H). ^{13}C NMR (150 MHz, $CDCl_3$): δ (ppm) = 155.82, 120.67, 117.19, 117.00, 39.46, 33.29, 32.97, 31.95. 29.72, 29.30, 28.85, 26.59, 22.08, 22.76, 14.18.

1.2.6. Synthesis of 1.2-bis(5-(2-butyloctyl)-4-fluorothiophen-2-yl)ethane-1,2-dione (7)

After dissolving **6** (16.42 mmol) in dry THF (50 ml) under a N_2 atmosphere, n-butyllithium (18.66 mmol, 2.5M in hexane) was added slowly at -78 °C. After stirring for 2 h at -78°C, the dispersion of lithium bromide (LiBr, 35,08 mmol) and cuprous bromide (CuBr, 16.42mmol) in dry THF (80 ml) was added slowly at 0 °C. After additional reaction time of 1 h, oxalyl chloride (7.46 mmol) was slowly added, and the reaction mixture was stirred overnight at room temperature. Once the reaction was completed, the mixture was poured into water and extracted with dichloromethane. The organic layers were separated and dried over magnesium sulfate and filtered. Solvents were removed under reduced pressure, and the crude residue was purified by column chromatography with hexane/dichloromethane (15/1, v/v). Yield: 48%. ^{1}H NMR (600 MHz, $CDCl_3$): δ (ppm) = 7.74 (s, 2H), 2.76 (d, J = 6.54Hz 4H), 1.70 (s, 2H) 1.29-1.26 (m, 32H), 0.90-0.87 (m, 12H). ^{13}C NMR (150 MHz, $CDCl_3$): δ (ppm) = 179.73, 156.40, 154.70, 136.87, 125.82, 39.52, 33.31, 33.00, 31.90, 30.28, 29.63, 28.76, 26.54, 22.99, 14.10.

1.2.7. Synthesis of 2,3-bis(5-(2-butyloctyl)-4-fluorothiophen-2-yl)-6-fluoro-5,8-di(thiophen-2-yl)quinoxaline (9)

A mixture of 5-fluoro-4,7-di(thiophen-2-yl)benzo[c][1,2,5]thiadiazole (**8**, 0.63 mmol) and zinc powder (20 equiv., 12.56 mmol) in acetic acid (20 ml) was stirred at 80 °C for 4 h. Upon completion of the reaction, the mixture was filtered to remove zinc power and the filtrate was collected. After addition of 7 (0.63 mmol) to the filtrate, the solution was heated to reflux for overnight. The solution was cooled down to room temperature. The mixture was poured into water and extracted with dichloromethane. The organic layers were collected and dried over magnesium sulfate. Solvents were removed under reduced pressure. The crude residue was further purified by column chromatography with hexane and dichloromethane (10/1 = v/v).

Yield: 75%. ^{1}H NMR (600 MHz, $CDCl_3$): δ (ppm) = 7.96 (t, *J* = 1.5Hz, 1H), 7.91 (d, *J* = 13.08Hz 1H), 7.87-7.86 (m, 1H) 7.74 (s, 1H), 7.61 (dd, *J* = 1.02Hz, 10.08Hz 1H), 7.57 (dd, *J* = 1.02Hz, 10.08Hz 1H), 7.25-7.23 (m, 2H), 7.20 (dd, *J* = 4.02Hz, 10.08Hz 1H), 2.79-2.75 (m, 4H), 1.73-1.71 (m, 2H), 1.36-1.25 (m, 32H), 0.93-0.85 (m, 12H). ^{13}C NMR (150 MHz, $CDCl_3$): δ (ppm) = 159.91, 158.22, 156.44, 155.04, 154.74, 153.35, 144.21, 142.84, 138.10, 137.25, 135.09, 133.81, 132.00, 131.35, 130.58, 129.79. 129.08, 127.58, 126.97, 126.56, 125.93, 119.69, 119.42, 117.45, 39.56, 33.45, 33.04, 33.00, 32.00, 31.91, 30.40, 29.76, 28.88, 26.67, 23.11, 22.76, 14.24.

1.2.8. Synthesis of 5,8-bis(5-bromothiophen-2-yl)-2,3-bis(5-(2-butyloctyl)-4-fluorothiophen-2-yl)-6-fluoroquinoxaline (10)

A mixture of 9 (0.45 mmol) and NBS (0.98 mmol) in THF (30 ml) was stirred at room temperature for overnight. The solution was poured into water and extracted with dichloromethane. The organic layers weredried with magnesium sulfite and filtered. Solvents were removed under reduced pressure, and the residue was purified by the column chromatography on silica gel with hexane and dichloromethane (8/1 = v/v). Yield: 69% ^{1}H NMR (600 MHz, $CDCl_3$): δ (ppm) = 7.83 (d, *J* = 13.62Hz, 1H), 7.73 (d, *J* = 4.02Hz 1H), 7.54 (d, *J* = 4.02Hz 1H), 7.23 (d, *J* = 11.10Hz, 2H), 7.17 (d, *J* = 4.02Hz, 1H), 7.15 (d, *J* = 4.02Hz, 1H), 2.80 (dd, *J* = 4.02Hz, 13.08Hz 4H), 1.76-1.75 (m, 2H), 1.37-1.28 (m, 32H), 0.92-0.86 (m, 12H). ^{13}C NMR (150 MHz, $CDCl_3$): δ (ppm) = 159.76, 158.07, 155.02, 153.33, 144.40, 143.50, 137.84, 137.28, 134.61, 133.08, 130.83, 130.57, 129.28, 127.64, 127.01, 126.58, 119.96, 119.78, 119.66, 119.47, 118.34, 117.70, 116.02, 115.84, 39.44, 33.50, 33.10, 32.00, 29.80, 28.92, 26.71, 23.14, 22.77, 14.26. MALDI-TOF MS: mz calcd, 1007.043; found 1007.263 [M^+].

1.2.9. Synthesis of PB-QxF

In a Schlenk flask, benzodithiophene (BDT) monomer (**11**, 0.20 mmol), dibrominated quinoxaline monomer (**10**, 0.20 mmol) and $Pd(PPh_3)_4$ (3 mol%) were dissolved in dry toluene (10 ml). After N2 has been bubbled 15 min, the reaction mixture was heat to 90 °C and stirred for 2 d under a N_2 atmosphere. After the end of polymerization, 2-tributylstannylthiophene and 2-bromothiophene were consecutively added as end-capping agents with an interval of 3 h. The mixture was cooled down to room temperature and precipitated into methanol. The precipitated black solids were collected and further purified by Soxhlet extraction with methanol, acetone, hexane, and chloroform in sequence. The polymers in the chloroform faction were recovered by precipitation into methanol again. Finally, the polymer was dried in a vacuum oven at 50 °C. Yield: 70%. ^{1}H NMR (600 MHz, $CDCl_3$): δ (ppm) = 7.51-7.27 (br, 5H), 7.20-7.06 (br, 3H), 7.06-6.80 (br, 5H), 3.03-2.67 (br, 8H), 1.83-1.63 (br, 4H), 1.49-0.78 (br, 72H). Molecular weight by GPC: number-average molecular weight (M_n) = 52.39 KDa, polydispersity index (PDI) = 1.98. Elemental analysis: calcd (%) for C: 69.06%, H: 7.00%, N: 1.96%, S: 17.99%, found: C: 69.84%, H: 7.10%, N: 1.67%, S: 19.47%.

1.2.10. Synthesis of PBF-QxF

The synthetic procedure of PBF-QxF was the same as the method for the preparation of PB-QxF described above. BDT monomer of **12** and **10** were used as monomers. Yield: 80% . ^{1}H NMR (400 MHz, $CDCl_3$): δ (ppm) = 7.57-.7.46 (br, 1H), 7.45-7.38 (br, 1H), 7.37-7.28 (br, 3H), 7.18-7.05 (br, 3H), 7.05- 6.84 (br, 3H), 2.92-2.72 (br, 8H), 1.70-1.65 (br, 4H), 1.49-1.16 (br, 48H). 1.15-0.68 (br, 24H). Molecular weight by GPC: M_n = 58.92 KDa, PDI = 2.16. Elemental analysis: calcd (%) for C: 67.36%, H: 6.69%, N: 1.92%, S: 17.54%, found: C:

67.87%, H: 6.68%, N: 1.68%, S: 15.13%.

2. Instruments

^{1}H and ^{13}C NMR spectra were measured with a JEOL JNM ECP-400 spectrometer. Matrix-assisted laser desorption/ionization time-of-flight (MALDI-TOF) analyses were carried out using an Bruker Ultraflex spectrometer. GPC measurements were conducted on an Agilent 1200 series instrument in the presence of THF eluent. Thermogravimetic analysis (TGA) was performed using a TA Instrument Q200 at a heating rate of 10 °C min^{-1} under N_2. UV-Vis spectra were recorded using a JASCO V-530 spectrometer. CV analyses were carried out using a VersaSTAT3 potentiostat (Princeton Applied Research), with tetrabutylammonium hexafluorophosphate (Bu_4NPF_6, 0.1 M) electrolyte in acetonitrile. A glassy carbon electrode coated with polymers and a platinum wire were used as a working and counter electrode, respectively. A silver wire was used as pseudo-reference electrode with a ferrocene/ferrocenium external standard. Grazing incidence wide angle X ray scattering (GIWAXS) measurements were performed using a synchrotron radiation at the Pohang Accelerator Laboratory (PAL), Republic of Korea. Atomic force microscopy(AFM) images were obtained from Bruker Nanoscope IV microscope operated in tapping mode.

3. Fabrication and analysis of organic photovoltaic devices

3.1. Fabrication and analysis of lab-scale PSC on glass substrate

BHJ PSCs with quinixaline-based polymers as the electron donor and Y6 as the acceptor were fabricated in an inverted type device with a structure of ITO/ZnO/Polymer:Y6/MoO_3/Ag. All the devices were manufactured according the following procedures; 1) the glass/ITO substrate was cleaned with detergent, and then ultrasonicated in the mixed solvent of acetone/isopropyl alcohol. Subsequently, the substrate was dried in an oven at 80 °C overnight. 2) ZnO film was prepared by spin-coating of diethylzinc precursor solution in THF (1:2, v/v) at 3500 rpm for 25 s followed by thermal annealing at 130 °C for 30 min. 3) The active layer was fabricated by spin-coating at 3000 rpm using a chloroform solution of polymeric donor and Y6 acceptor with 1 vol% 1-CN additive on the top of ZnO layer in a nitrogen-filled glove box. 4) a 7-nm-thick MoO3 layer and 100-nm-thick layer of Ag were consecutively deposited on the top of the active layer by thermal evaporation. The area of the deposited Ag electrode was controlled to 9 mm^2. Photovoltaic characteristics of the device were analyzed by using a solar simulator equipped with a Keithley 2635A source measurement under AM 1.5G illumination at 100 $mWcm^{-2}$. The monochromic light intensity was calibrated using a Si photodiode and chopped at 100 Hz. Field-emission transmission electron microscopy images were taken by using a FEI Tecnai G2 F20 X-twin microscope. The active layer of the device were separated by using the aqueous solution of hydrogen fluoride and supported on Cu grid.

3.2 Fabrication and analysis of R2R based organic photovoltaics

R2R-processed PSCs cells were fabricated with an inverted structure (Transparent conductive electrode (TCE)/ZnO NPs/PBF_Qx1F:Y6/MoO_3/Ag). The experiment was carried out using a commercial R2R coater (Mini Labo, Yasui Seki) combined with the customized slot die set-up. A ZnO NPs solution (Infinify PV, 5.6 % (w/v) in IPA) was slot die coated on a commercially available flexible transparent conductive substrate (Solutia OPV8, 8 Ω sq^{-1}, patterned by MekoPrint) and annealed on a curved hot plate set at 120 °C. The coating was carried out at the minimum speed (20 cm/min) with the solution feed rate of 10 μL/min. Based on 26 cm^2/min (1.3 cm width × 20 cm length) coating area, coating volume was 0.385 μl/cm^2 which is equivalent to 3.85 μm of wet film thickness. Then, a mixed solution of PBF-QxF:Y6

(1:1.5, w/w) in *o*-dichlorobenzene (10 mg/ml) was slot die-coated. A substrate temperature/head temperature of 130/90 °C and a coating speed (30 cm/min) were used. To find the optimal thickness, the solution feeds were regularly changed in the range of 10–90 μL/min (wet film thickness: 2.56–23.08 μm) using a programmable syringe pump (NEMESYS). The films were cut to 11 cm length for metal evaporation. All printing experiments and sample preparation were carried out in air. For the fabrication of top electrodes, the samples were transferred to a thermal evaporator. A 10 nm MoO_3 (Sigma-Aldrich) layer and a 100 nm Ag (KJ Lesker) layer were thermally deposited with a shadow mask to make a 14 mm^2 active area. The *J–V* characteristics of the R2R-processed PSCs were characterized using Keithley 2400 source measurement unit under AM 1.5G solar irradiation. The light was calibrated using a secondary reference cell (Hamamatsu S1133, with KG-5 filter, 2.8 × 2.4 mm^2 of photosensitive area), which was pre-calibrated by a certified reference cell (PV Measurements, certified by NREL) under 1000 W m^{-2} AM 1.5G illumination from an Oriel AAA solar simulator fitted with a 1000 W Xe lamp. Light intensity was constantly confirmed by the secondary reference cell just before the measurement.

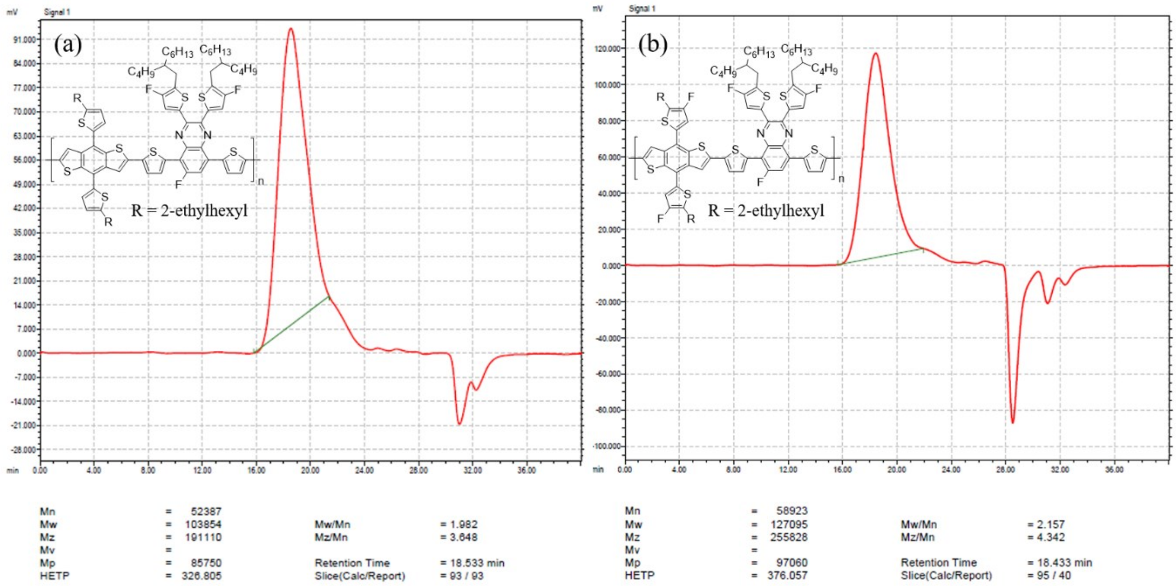

```
Mn      =    52387
Mw      =   103854      Mw/Mn                = 1.982
Mz      =   191110      Mz/Mn                = 3.648
Mv      =
Mp      =    85750      Retention Time       = 18.533 min
HETP    =  326.805      Slice(Calc/Report)   = 93 / 93
```

```
Mn      =    58923
Mw      =   127095      Mw/Mn                = 2.157
Mz      =   255828      Mz/Mn                = 4.342
Mv      =
Mp      =    97060      Retention Time       = 18.433 min
HETP    =  376.057      Slice(Calc/Report)   = 95 / 40
```

Figure S1. GPC curves of (a) PB-QxF and (b) PBF-QxF recorded at room temperature with THF eluent.

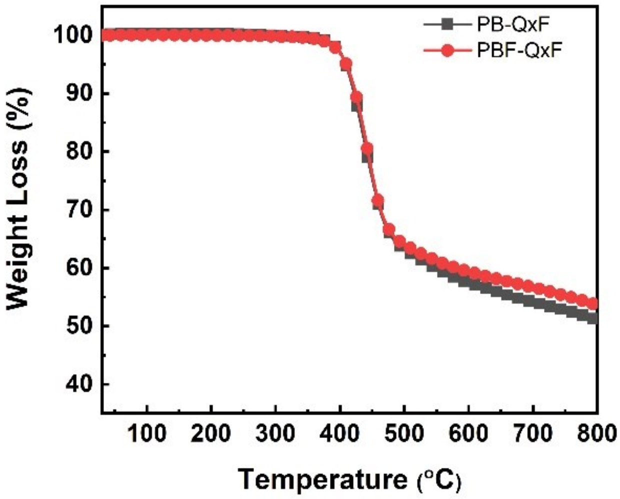

Figure S2. TGA thermograms of PB-QxF and PBF-QxF at a heatring rate of 10 ºC/min under N_2.

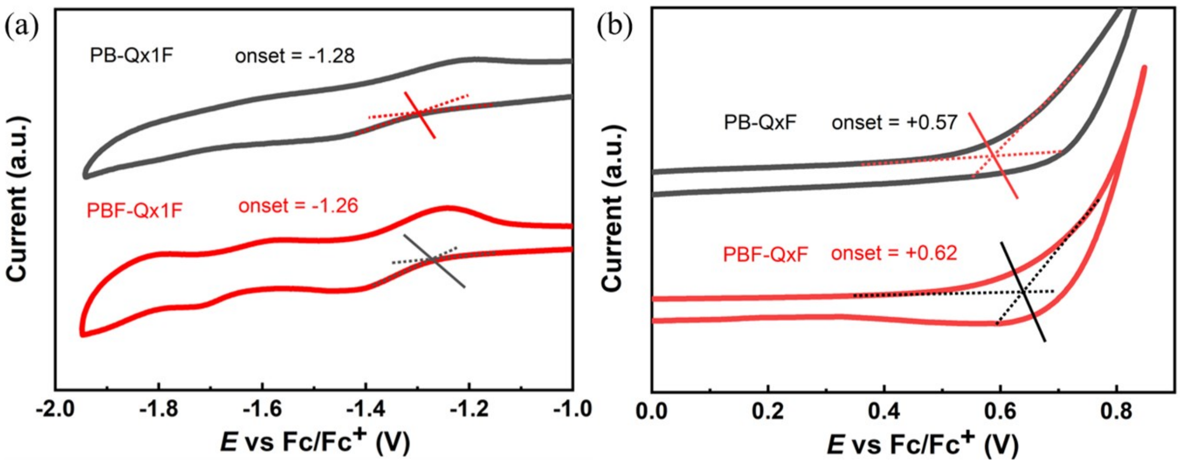

Figure S3. Cyclic voltammograms of (a) the reduction cycles and (b) the oxidation cycles of PB-QxF and PBF-QxF.

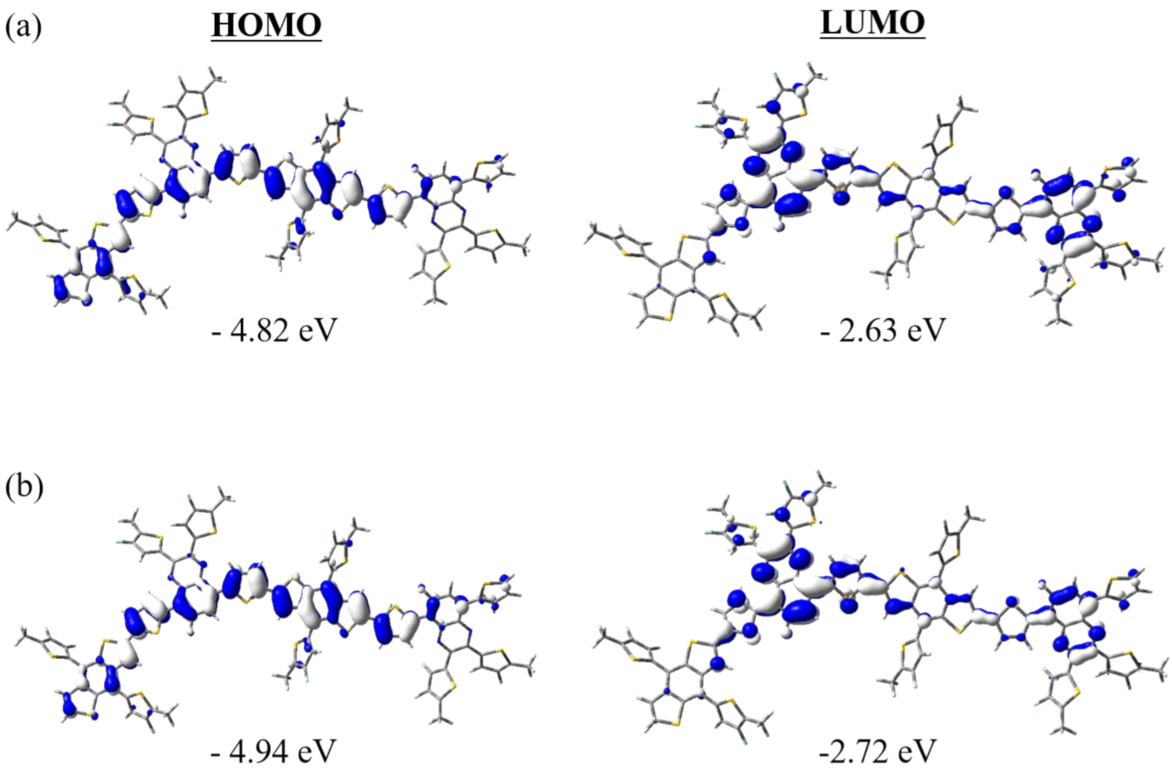

Figure S4. Frontier molecular orbitals of two-repeating unit with theoretical HOMO/LUMO energy levels at the B3LYP/6-31G** level for (a) PB-QxF and (b) PBF-QxF.

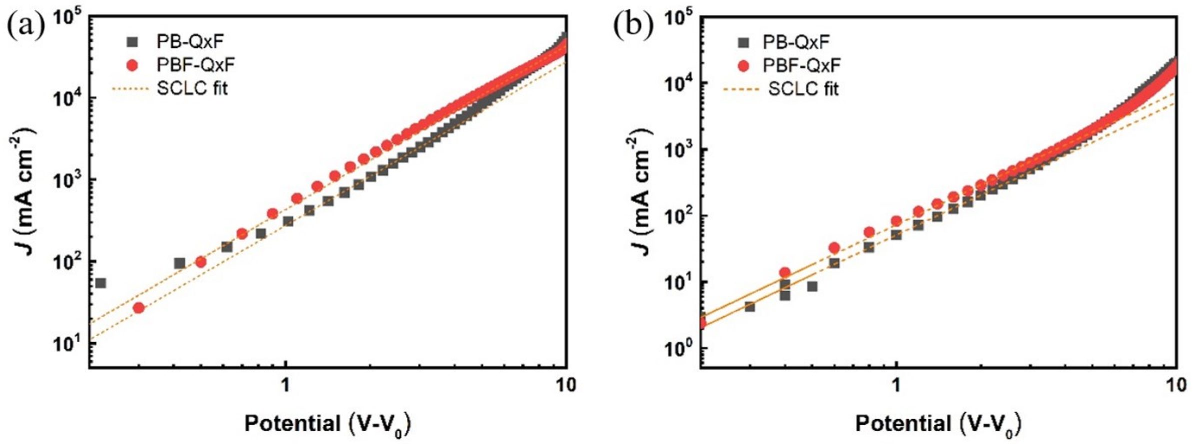

Figure S5. Current density vs. voltage curves of (a) hole- and (b) electron-only devices based on PB-QxF (square) and PBF-QxF (circle).

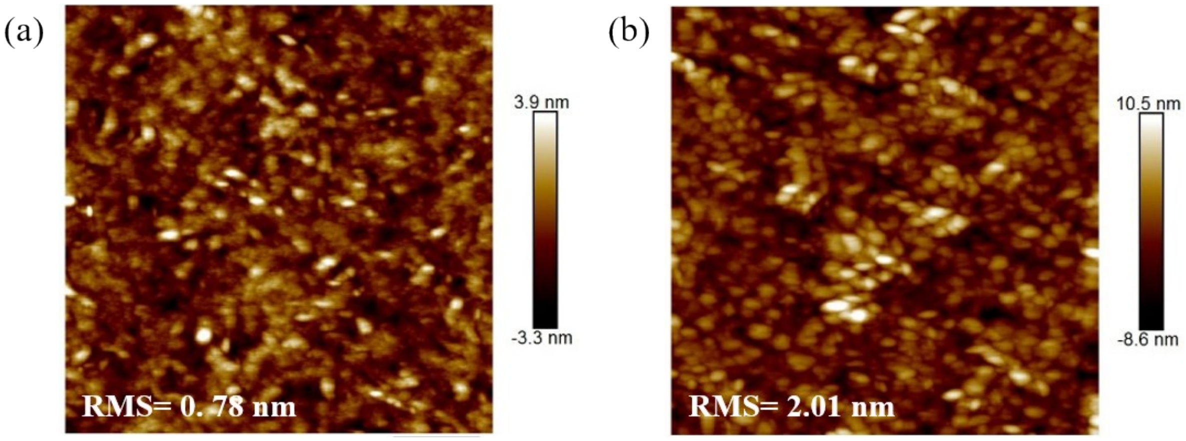

Figure S6. AFM images of the active layers based on (a) PB-QxF and (b) PBF-QxF with RMS value. The size of all images is 3.0 μm × 3.0 μm.

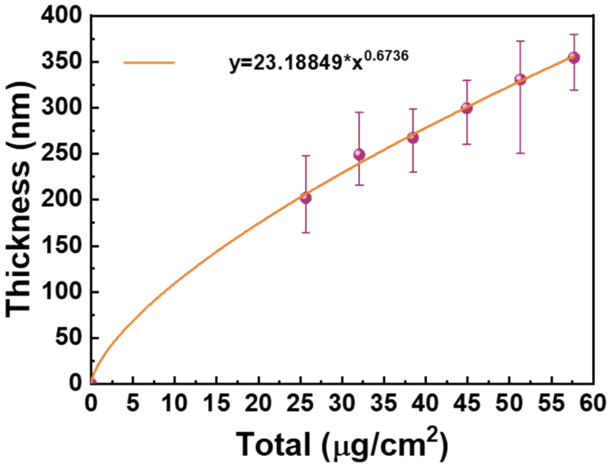

Total (μg/cm^2)	Thickness[a] (nm)	Thickness[c] (nm)*
57.69	354.26	356.09
51.28	330.54	328.93
44.87	299.42	300.63
38.46	267.32	270.99
32.05	249.12	239.67
25.64	202.01	206.22
19.23	NA[b]	169.89
12.82	NA[b]	129.29
6.41	NA[b]	81.06

[a] Measured by surface profiler
[b] Not applicable for surface profiler (The thin film on flexible substrate can be easily damaged during the measurement)
[c] Predicted thickness given by Allometric equation

Figure S7. The relationship between the deposited concentration and the thickness of the active layer in R2R slot die coated PSCs.

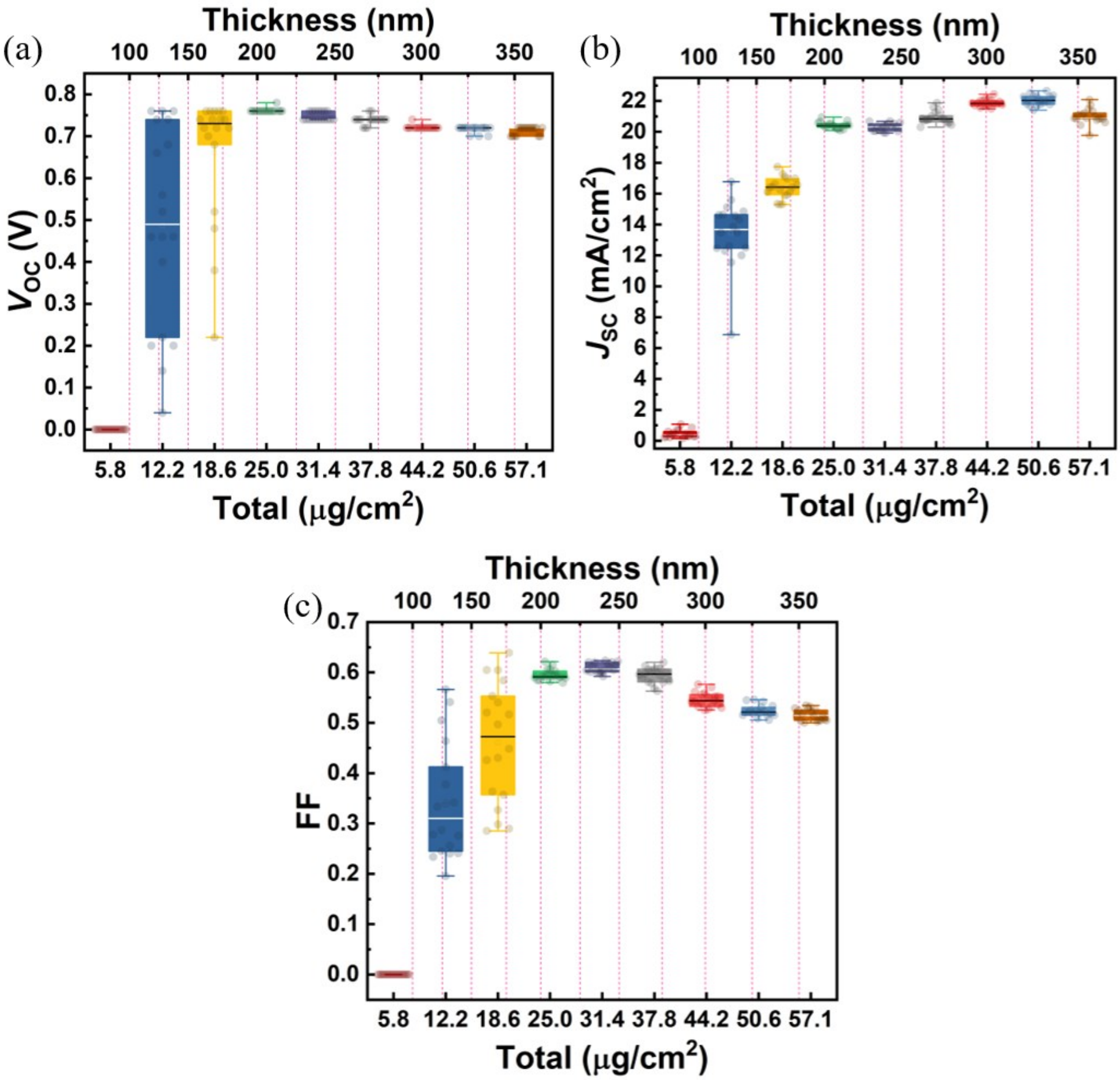

Figure S8. (a) V_{OC}, (b) J_{SC} and (c) FF variations of R2R slot die coated PSCs with different active layer thickness.

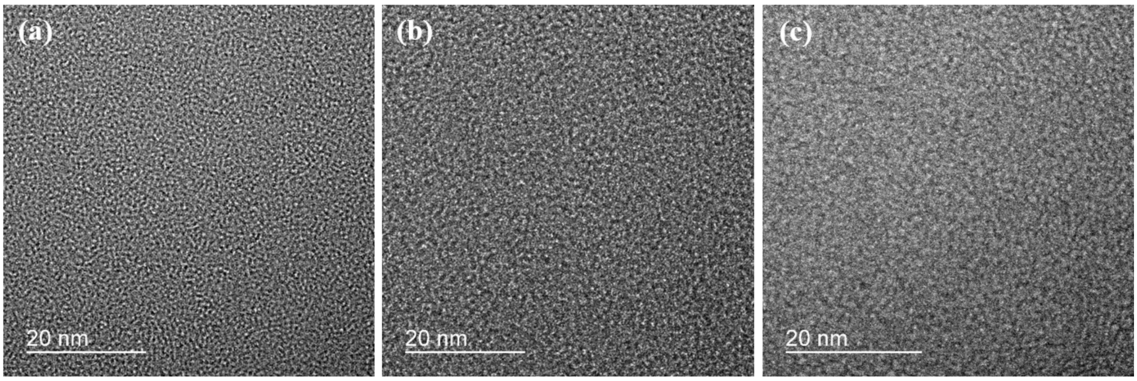

Figure S9. Field-emission transmission electron microscope images of the active layers processed by R2R Slot die coating with different concentrations of (a) 6.41 μg/cm^2 (b) 25.6 μg/cm^2, and (c) 57.7 μg/cm^2.

Table S1. Summary of optical and electrochemical properties of PB-QxF and PBF-QxF.

Polymer	$\lambda_{max}^{solution}$ (nm)	λ_{max}^{film} (nm)	$E_{g,OPT}$ (eV)[a]	HOMO (eV)[b]	LUMO (eV)[c]	$E_{g,CV}$ (eV)[d]
PB-QxF	438, 596	436, 616	-1.63	- 5.37	- 3.52	-1.85
PBF-QxF	443. 610	450, 630	-1.66	- 5.42	- 3.54	-1.88

[a] Estimated from the λ_{edge}. [b] Estimated from the oxidation onset potential of CV curve based on the equation of $E_{HOMO} = -(E_{OX} + 4.80)$ eV. [c] Estimated from the reduction onset potential in CV curves based on the equation of $E_{LUMO} = -(E_{RED} + 4.80)$ eV. [d] Calculated from the HOMO and LUMO energy level.

Table S2. Summary of device parameter based on polymers:Y6 blend.

Donor	Blend ratio (polymer:Y6)	Additive (1-CN)[a]	solvent	Annealing (110°C/5m)	J_{SC} (mA cm^{-2})	V_{OC} (V)	FF	PCE (%)
PB-Qx1F	1:1	x	CF[c]	x	21.75	0.82	0.50	8.95
		x		o	23.36	0.80	0.52	9.67
	1:1.5	x	CF	x	23.41	0.82	0.49	9.30
		x		o	24.76	0.79	0.52	10.13
	1:2	x	CF	x	21.25	0.80	0.47	8.06
		x		o	22.46	0.78	0.48	8.46
	1:1.5	1%	CF	x	23.42	0.82	0.55	10.64
		1%		**o**	**24.43**	**0.79**	**0.58**	**10.99**
PBF-Qx1F	1:1	x	CF	x	22.89	0.87	0.60	11.98
		x		o	24.77	0.84	0.61	12.64
	1:1.5	x	CF	x	24.37	0.85	0.61	12.70
		x		o	25.24	0.84	0.61	12.94
	1:2	x	CF	x	22.85	0.85	0.62	11.97
		x		o	24.17	0.83	0.62	12.53
	1:1.5	1%	CF	x	23.09	0.83	0.68	13.01
		1%		**o**	**24.14**	**0.83**	**0.69**	**13.96**
	1:1.5	1% DIO[b]	CF	x	24.38	0.80	0.67	13.18
		1% DIO		o	25.00	0.78	0.67	12.92

[a] 1-CN: 1-Chloronathphalene
[b] DIO: 1,8-Diiodooctane
[c] CF: Chloroform

Table S3. The recent hole and electron mobility data of PSCs based on Y6 acceptor with polymer donors.

Polymer	Hole mobility (μ_h) ($cm^2 V^{-1} s^{-1}$)	Electron Mobility (μ_e) ($cm^2 V^{-1} s^{-1}$)	$\mu_{h/}\mu_e$	ref
PBDB-T-SF	1.17×10^{-4}	2.18×10^{-4}	0.54	4
J52-FS	5.77×10^{-4}	2.72×10^{-4}	2.12	5
PE2	5.06×10^{-4}	1.07×10^{-4}	4.73	5
PBDB-T-H	7.3×10^{-4}	1.3×10^{-4}	5.62	6
PBDB-T-Br	7.5×10^{-4}	7.0×10^{-4}	1.07	6
PBDB-T-OMe	6.4×10^{-4}	5.8×10^{-4}	1.10	6
PBDB-T-T	1.7×10^{-4}	1.8×10^{-4}	0.94	6
J71	1.72×10^{-4}	1.94×10^{-5}	0.89	7
PE31	0.51×10^{-4}	0.85×10^{-5}	6.00	8
PE32	1.97×10^{-4}	2.08×10^{-5}	9.47	8
J52-Cl	3.57×10^{-4}	3.70×10^{-5}	9.65	8
PE4	8.04×10^{-4}	1.14×10^{-4}	7.05	8
P2F-EHP	1.18×10^{-4}	0.83×10^{-4}	1.42	9
PBiTPD	4.61×10^{-4}	2.42×10^{-4}	1.90	10
PM6	2.00×10^{-4}	5.90×10^{-4}	0.34	11
Pt0	6.7×10^{-4}	2.2×10^{-4}	3.05	12
Pt5	6.2×10^{-4}	3.3×10^{-4}	1.88	12
PTBT	4.8×10^{-5}	8.5×10^{-6}	5.65	13
PTBT-Cl	7.8×10^{-5}	6.5×10^{-5}	1.20	13
PTQ7(Qx)	0.48×10^{-5}			14
PTQ9(Qx)	1.20×10^{-5}			14
PTQ10(Qx)	3.12×10^{-5}			14
PTQ10(Qx)	3.26×10^{-3}	1.35×10^{-3}	2.41	15
PE61 (Qx)	1.18×10^{-4}	1.40×10^{-4}	0.84	16
PE62 (Qx)	1.76×10^{-4}	2.56×10^{-4}	0.69	16
PE63 (Qx)	1.96×10^{-4}	3.15×10^{-4}	0.62	16
PB-QxF	**6.7×10^{-4}**	**2.8×10^{-4}**	**2.39**	**This work**
PBF-QxF	**1.1×10^{-3}**	**7.4×10^{-4}**	**1.49**	**This work**

Table S4. Summary of GIWAXS results.

Films	Materials	GIWAXS parameters					
		Lamellar spacing (q_{xy} direction)		π-π stack (q_z direction)		π-π stack (q_{xy} direction)	
		q (Å^{-1})	d-spacing (Å)	q(Å^{-1})	d-spacing (Å)	q(Å^{-1})	d-spacing (Å)
Pristine film	PB-QxF	0.2676	23.48	1.607	3.910	1.611	3.900
	PBF-QxF	0.2676	23.48	1.649	3.810	1.593	3.940
	Y6	0.2898	21.68	1.726	3.640	-	
BHJ Film	PB-QxF:Y6	0.2742	22.91	1.707	3.680	1.649	3.810
	PBF-QxF:Y6	0.2698	23.29	1.707	3.680	1.647	3.815
BHJ with Additive film	PB-QxF:Y6 (1-CN)	0.2720, 0.4054	23.10, 15.50	1.719	3.655	1.613, 1.730	3.895, 3.632
	PBF-QxF:Y6 (1-CN)	0.2609, 0.4320	24.08, 14.54	1.767	3.556	1.653, 1.728	3.801, 3.636

Table S5. Summary of photovoltaic properties of R2R processed PSCs based on PBF-QxF:Y6 active layer.

Thickness	Head (^{o}C)	Bed (^{o}C)	Line Speed (m/s)	V_{OC} (V)	J_{SC} (mA/cm^2)	FF	PCE (%)
6.4	90	130	0.30	0.00 (0.00±0.00)	1.07 (0.45±0.92)	0.00 (0.00±0.00)	0.00 (0.00±0.00)
12.8				0.76 (0.49±0.72)	16.77 (13.42±9.90)	0.54 (0.34±0.37)	6.90 (2.71±6.85)
19.2				0.76 (0.66±0.54)	17.74 (16.38±2.45)	0.60 (0.46±0.35)	8.15 (5.24±6.98)
25.6				**0.76** **(0.76±0.02)**	**20.39** **(20.58±0.86)**	**0.62** **(0.59±0.04)**	**9.63** **(9.21±0.62)**
32.1				0.76 (0.75±0.02)	20.53 (20.30±0.76)	0.61 (0.61±0.03)	9.55 (9.24±0.51)
38.5				0.74 (0.74±0.04)	20.86 (20.91±1.58)	0.61 (0.59±0.06)	9.39 (9.18±0.47)
44.9				0.72 (0.72±0.02)	21.71 (21.87±0.95)	0.58 (0.55±0.05)	9.01 (8.61±0.75)
51.3				0.72 (0.72±0.02)	21.78 (22.04±1.26)	0.54 (0.52±0.04)	8.54 (8.27±0.61)
57.7				0.72 (0.71±0.02)	22.08 (20.99±2.31)	0.53 (0.52±0.03)	8.49 (7.72±1.17)

Table S6. Summary of the performances of other R2R processed devices

Active layer	Additive	Year	J_{sc} (mA cm^{-2})	V_{oc} (V)	FF	PCE (%)	Ref.
PBDTTTz-4:PCBM	O **1-chloronaphthalene**	2015	17.80	13.1	0.48	3.8	17
PTB7:PC$_{71}$BM	O **1,8-diiodooctane**	2017	15.91	0.76	0.63	7.32	18
PPDT2FBT:PC$_{71}$BM	X	2018	15.61	0.74	0.60	7.06	19
PTB7-Th:PC71BM: COi8DFIC	O **1,8-diiodooctane**	2019	23.50	0.68	0.60	9.57	20
PBF-QxF:Y6	**X**	**2020**	**20.39**	**0.76**	**0.62**	**9.63**	**This work**

4. References

1 W. T. Neo, K. H. Ong, T. T. Lin, S. J. Chua and J. Xu, *J. Mater. Chem. C*, 2015, **3**, 5589–5597.

2 L. Huo, S. Zhang, X. Guo, F. Xu, Y. Li and J. Hou, *Angew. Chemie - Int. Ed.*, 2011, **50**, 9697–9702.

3 M. Zhang, X. Guo, W. Ma, H. Ade and J. Hou, *Adv. Mater.*, 2015, **27**, 4655–4660.

4 Y. Chang, T. Lau, M. Pan, X. Lu, H. Yan and C. Zhan, *Mater. Horizons*, 2019, **6**, 2094–2102.

5 Y. Chen, Y. Geng, T. Ailing, X. Wnag, Y. Sun and E. Zhou, *Chem. Commun.*, 2019, **55**, 6708–6710.

6 F. Liu, C. Xiao, G. Feng, C. Li, Y. Wu, E. Zhou and W. Li, *ACS Appl. Mater. Interfaces*, 2020, **12**, 6151–6158.

7 X. Ma, Q. An, O. A. Ibraikulov, P. L´evˆeque, T. Heiser, N. Leclerc, X. Zhang and F. Zhang, *J. Mater. Chem. A*, 2020, **8**, 1265–1272.

8 A. Tang, Q. Zhang, M. Du, G. Li, Y. Geng, J. Zhang, Z. Wei, X. Sun, E. Zhou, Q. Zhang, M. Du, G. Li, Y. Geng, J. Zhang, Z. Wei, X. Sun and E. Zhou, *Macromolecules*, 2019, **52**, 6227–6233.

9 B. Fan, D. Zhang, M. Li, W. Zhong, Z. Zeng, L. Ying, F. Huang and Y. Cao, *Sci. CHINA Chemstiry*, 2019, **62**, 746–752.

10 J. Zhao, Q. Li, S. Liu, Z. Cao, X. Jiao, Y. Cai and F. Huang, *ACS Energy Lett.*, 2020, **5**, 367–375.

11 J. Yuan, Y. Zhang, L. Zhou, G. Zhang, H.-L. Yip, T.-K. Lau, X. Lu, C. Zhu, H. Peng, P. A. Johnson, M. Leclerc, Y. Cao, J. Ulanski, Y. Li and Y. Zou, *Joule*, 2019, **3**, 1140–

1151.

12 X. Xu, K. Feng, Z. Bi, W. Ma, G. Zhang and Q. Peng, *Adv. Mater.*, 2019, **31**, 1901872.

13 P. Chao, H. Chen, Y. Zhu, N. Zheng, H. Meng and F. He, *Macromolecules*, 2019, **53**, 165–173.

14 C. Sun, F. Pan, S. Chen, R. Wang, R. Sun, Z. Shang, B. Qiu, J. Min, M. Lv, L. Meng, C. Zhang, M. Xiao, C. Yang and Y. Li, *Adv. Mater.*, 2019, **31**, 1905480.

15 Y. Wu, Y. Zheng, H. Yang, C. Sun, Y. Dong, C. Cui, H. Yan and Y. Li, *Sci. CHINA Chemstiry*, 2019, **63**, 265–271.

16 J. Yang, P. Cong, L. Chen, X. Wang, J. Li, A. Tang, B. Zhang, Y. Geng and E. Zhou, *ACS Macro Lett.*, 2019, **8**, 743–748.

17 M. Helgesen, J. E. Carlé, A. Gisele, R. Benatto, R. R. Søndergaard, M. Jørgensen, E. Bundgaard and F. C. Krebs, *Adv. Energy Mater.*, 2015, **5**, 1401996.

18 Y. C. Huang, H. C. Cha, C. Y. Chen and C. S. Tsao, *Prog. Phtovoltaics Res. Appl.*, 2017, **25**, 928–935.

19 S. Song, K. T. Lee, C. W. Koh, H. Shin, M. Gao, H. Y. Woo, D. Vak and J. Y. Kim, *Energy Environ. Sci.*, 2018, **11**, 3248–3255.

20 J. Lee, Y. Seo, S. Kwon, D. Kim, S. Jang, H. Jung, Y. Lee, H. Weerasinghe, T. Kim, J. Y. Kim, D. Vak and S. Na, *Adv. Energy Mater.*, 2019, **9**, 1901805.

<Appendix – ^{1}H & ^{13}C NMR spectra of all new materials>

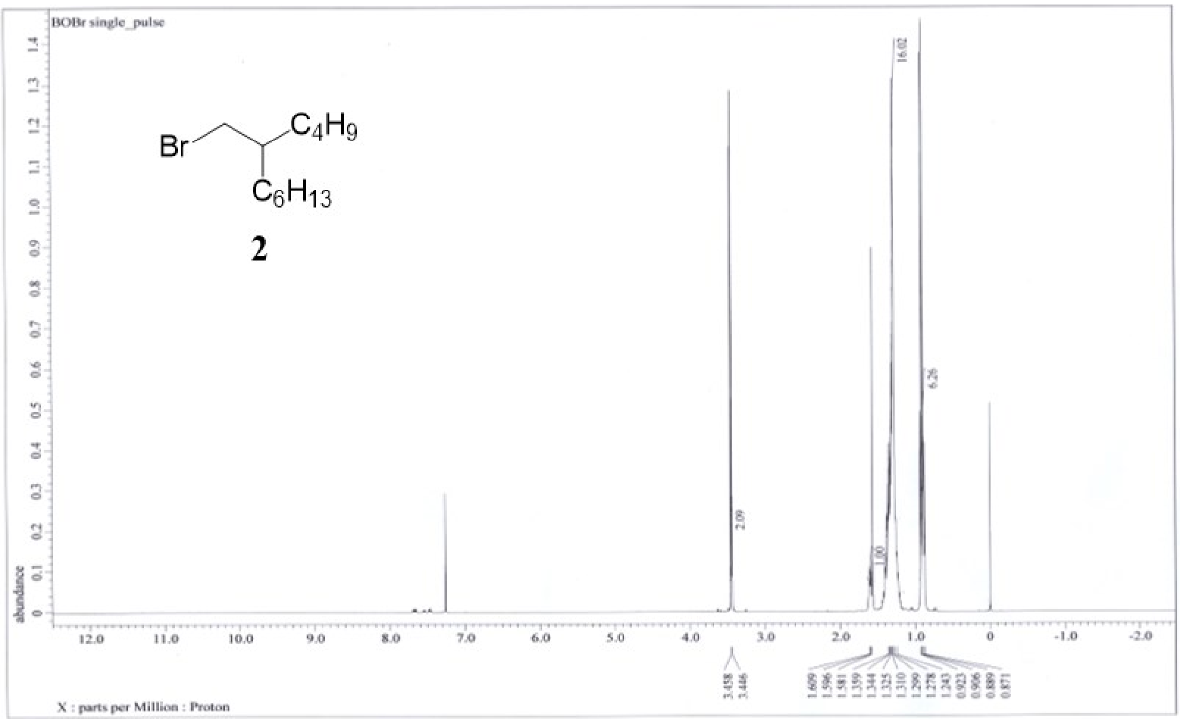
BOBr single_pulse
Br
C_4H_9
C_6H_{13}
2
abundance
0
0.1
0.2
0.3
0.4
0.5
0.6
0.7
0.8
0.9
1.0
1.1
1.2
1.3
1.4
2.09
1.00
16.02
6.26
12.0
11.0
10.0
9.0
8.0
7.0
6.0
5.0
4.0
3.0
2.0
1.0
0
-1.0
-2.0
3.458
3.446
1.609
1.596
1.581
1.359
1.344
1.325
1.310
1.299
1.278
1.243
0.923
0.906
0.889
0.871
X : parts per Million : Proton

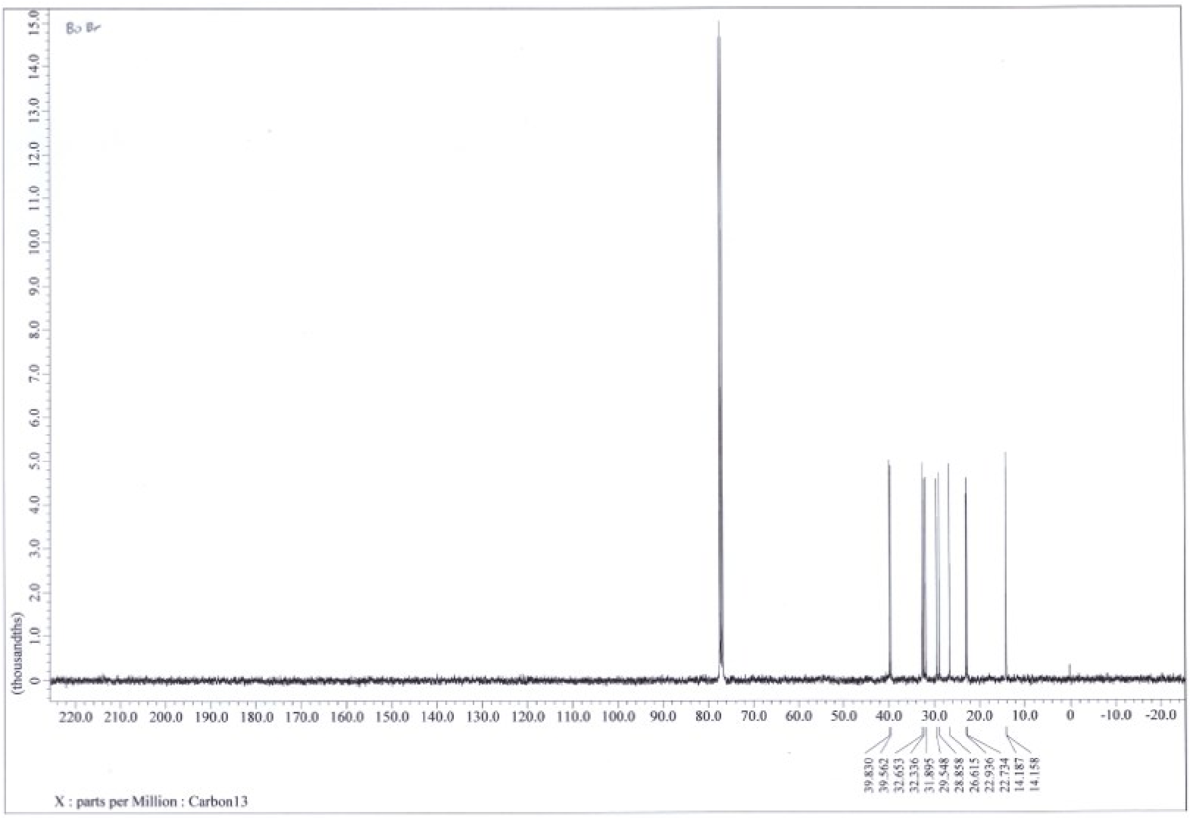
Bo Br
(thousandths)
0
1.0
2.0
3.0
4.0
5.0
6.0
7.0
8.0
9.0
10.0
11.0
12.0
13.0
14.0
15.0
220.0
210.0
200.0
190.0
180.0
170.0
160.0
150.0
140.0
130.0
120.0
110.0
100.0
90.0
80.0
70.0
60.0
50.0
40.0
30.0
20.0
10.0
0
-10.0
-20.0
39.830
39.562
32.653
32.336
31.895
29.548
28.858
26.615
22.936
22.734
14.187
14.158
X : parts per Million : Carbon13

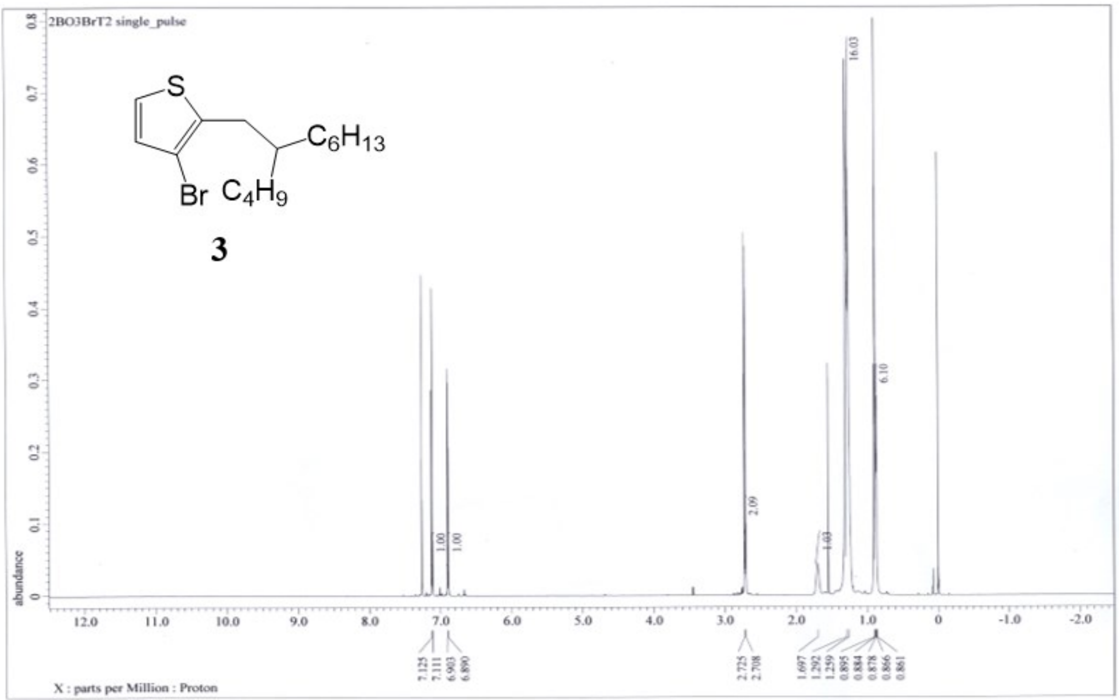
2BO3BrT2 single_pulse
S
C6H13
Br C4H9
3
abundance
0.8
0.7
0.6
0.5
0.4
0.3
0.2
0.1
0
1.00
1.00
2.09
1.03
16.03
6.10
12.0
11.0
10.0
9.0
8.0
7.0
6.0
5.0
4.0
3.0
2.0
1.0
0
-1.0
-2.0
7.125
7.111
6.903
6.890
2.725
2.708
1.697
1.292
1.259
0.895
0.884
0.878
0.866
0.861
X : parts per Million : Proton

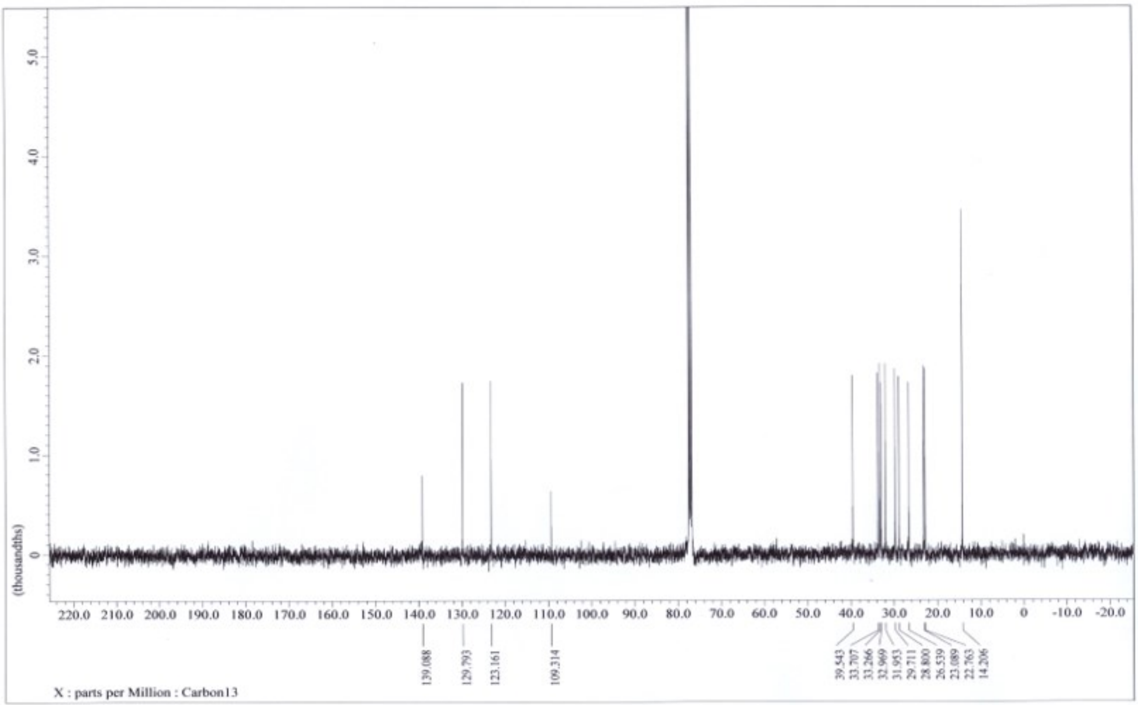
(thousandths)
5.0
4.0
3.0
2.0
1.0
0
220.0
210.0
200.0
190.0
180.0
170.0
160.0
150.0
140.0
130.0
120.0
110.0
100.0
90.0
80.0
70.0
60.0
50.0
40.0
30.0
20.0
10.0
0
-10.0
-20.0
139.088
129.793
123.161
109.314
39.543
33.707
33.266
32.969
31.953
29.711
28.800
26.539
23.089
22.763
14.206
X : parts per Million : Carbon13

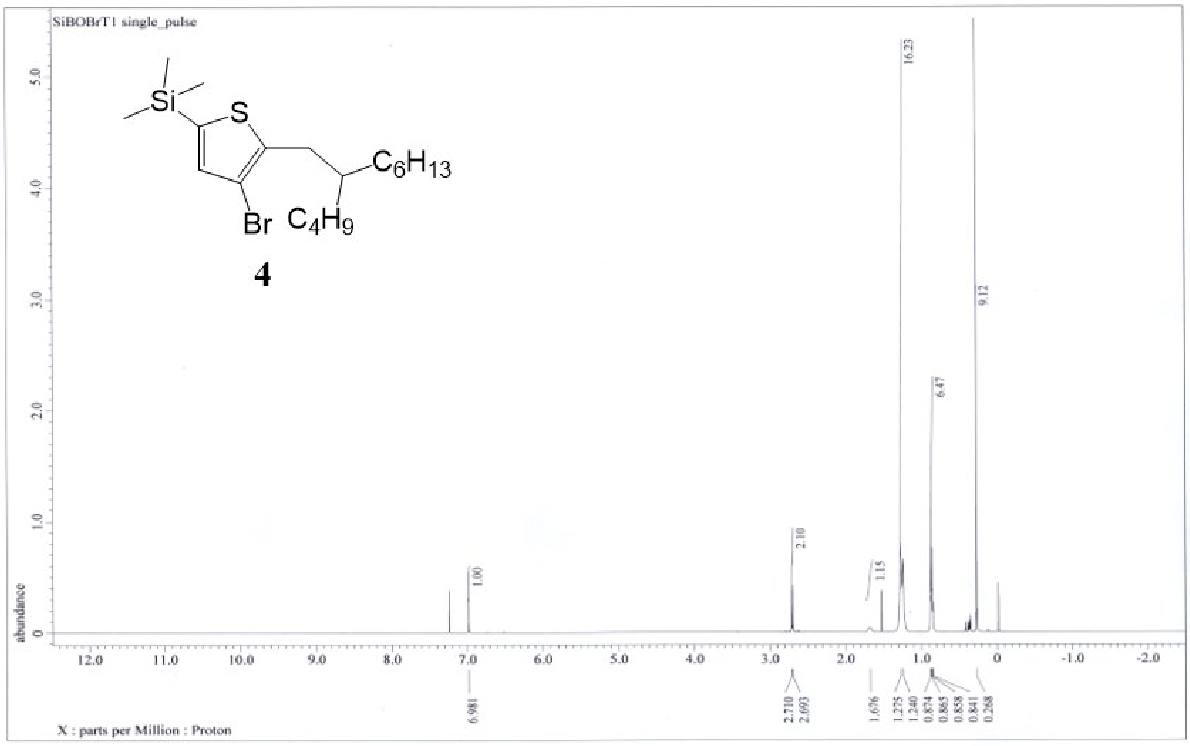
SiBOBrT1 single_pulse
Si
S
C6H13
Br
C4H9
4
abundance
5.0
4.0
3.0
2.0
1.0
0
16.23
9.12
6.47
2.10
1.15
1.00
12.0 11.0 10.0 9.0 8.0 7.0 6.0 5.0 4.0 3.0 2.0 1.0 0 -1.0 -2.0
6.981
2.710
2.693
1.676
1.275
1.240
0.874
0.865
0.858
0.841
0.268
X : parts per Million : Proton

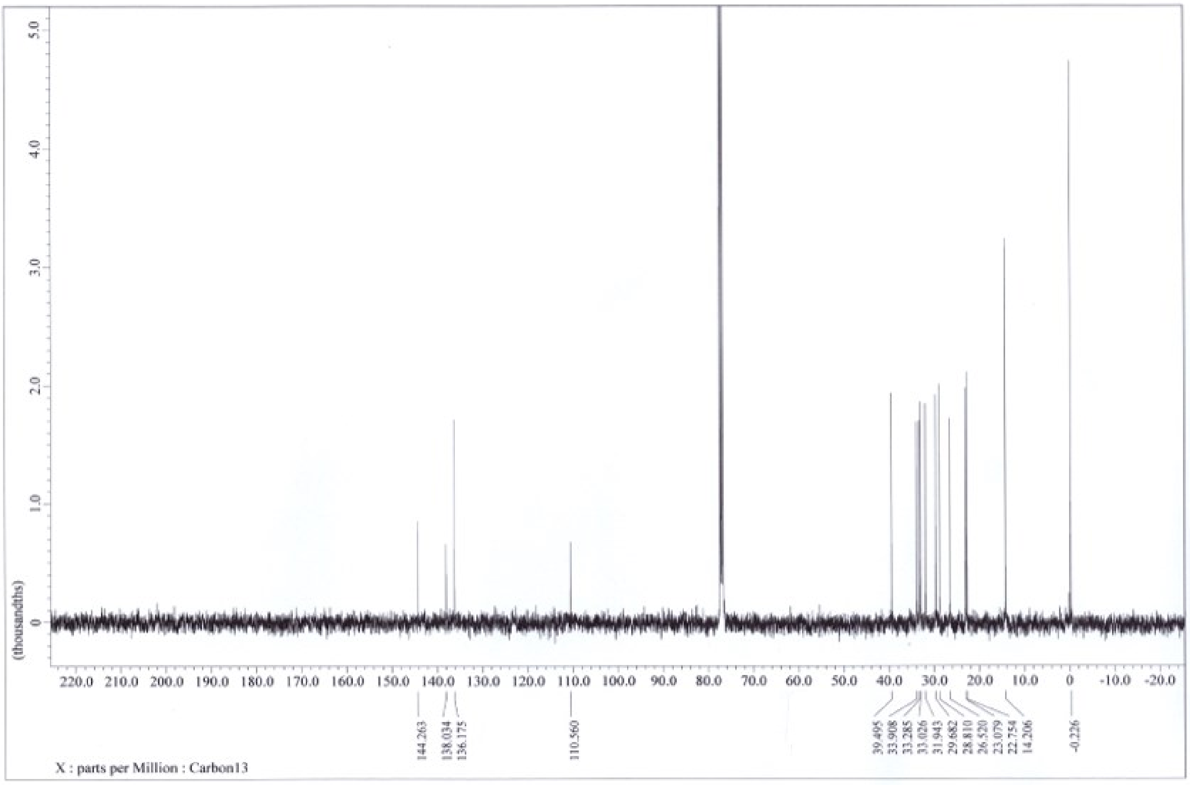
(thousandths)
5.0
4.0
3.0
2.0
1.0
0
220.0 210.0 200.0 190.0 180.0 170.0 160.0 150.0 140.0 130.0 120.0 110.0 100.0 90.0 80.0 70.0 60.0 50.0 40.0 30.0 20.0 10.0 0 -10.0 -20.0
144.263
138.034
136.175
110.560
39.495
33.908
33.285
33.026
31.943
29.682
28.810
26.520
23.079
22.754
14.206
-0.226
X : parts per Million : Carbon13

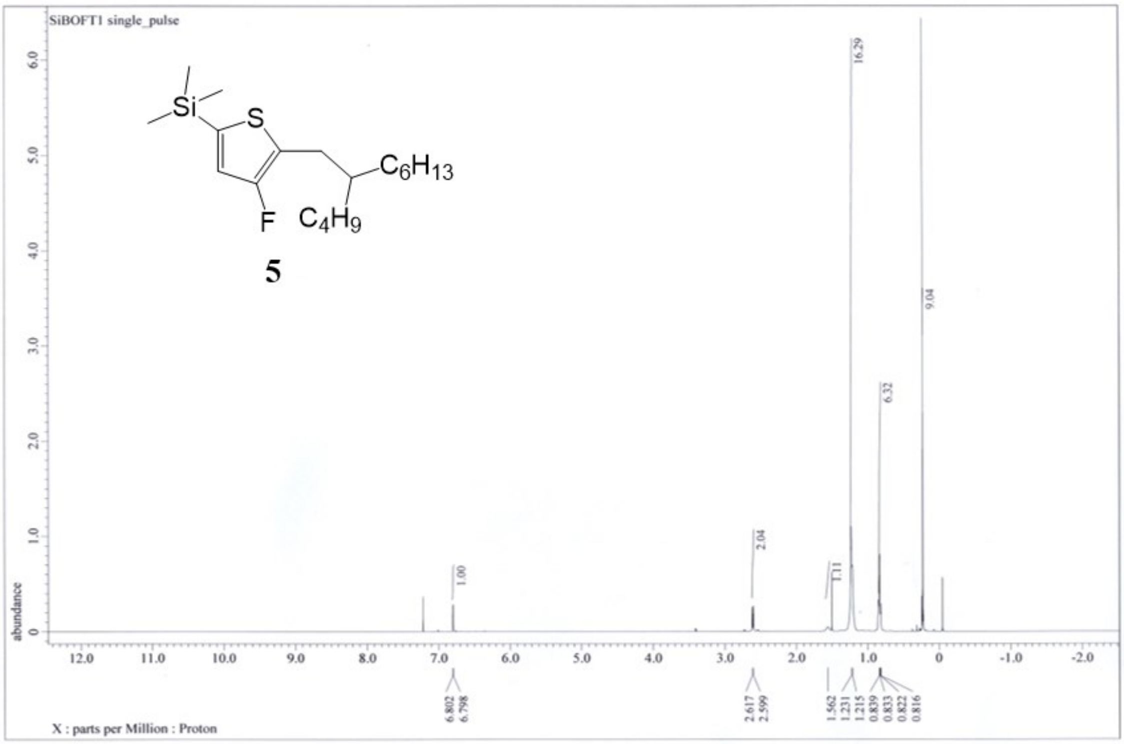
SiBOFT1 single_pulse
Si
S
F
C_6H_{13}
C_4H_9
5
abundance
16.29
9.04
6.32
2.04
1.11
1.00
6.802
6.798
2.617
2.599
1.562
1.231
1.215
0.839
0.833
0.822
0.816
X : parts per Million : Proton

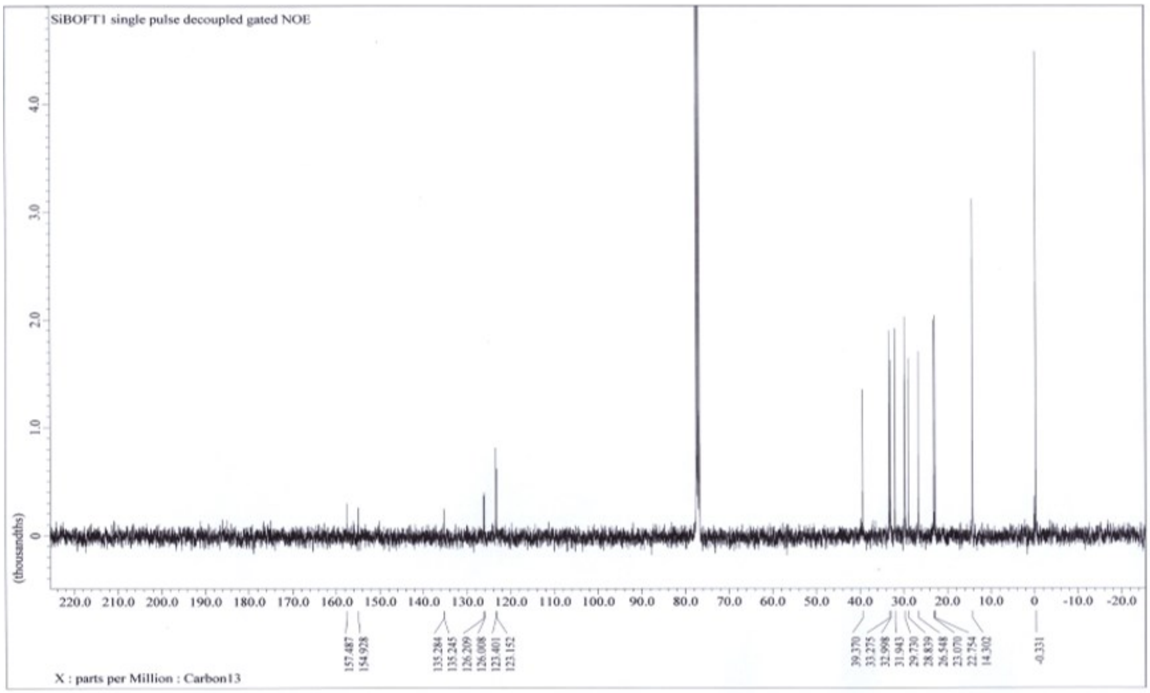
SiBOFT1 single pulse decoupled gated NOE
(thousandths)
157.487
154.928
135.284
135.245
126.209
126.008
123.401
123.152
39.370
33.275
32.998
31.943
29.730
28.839
26.548
23.070
22.754
14.302
-0.331
X : parts per Million : Carbon13

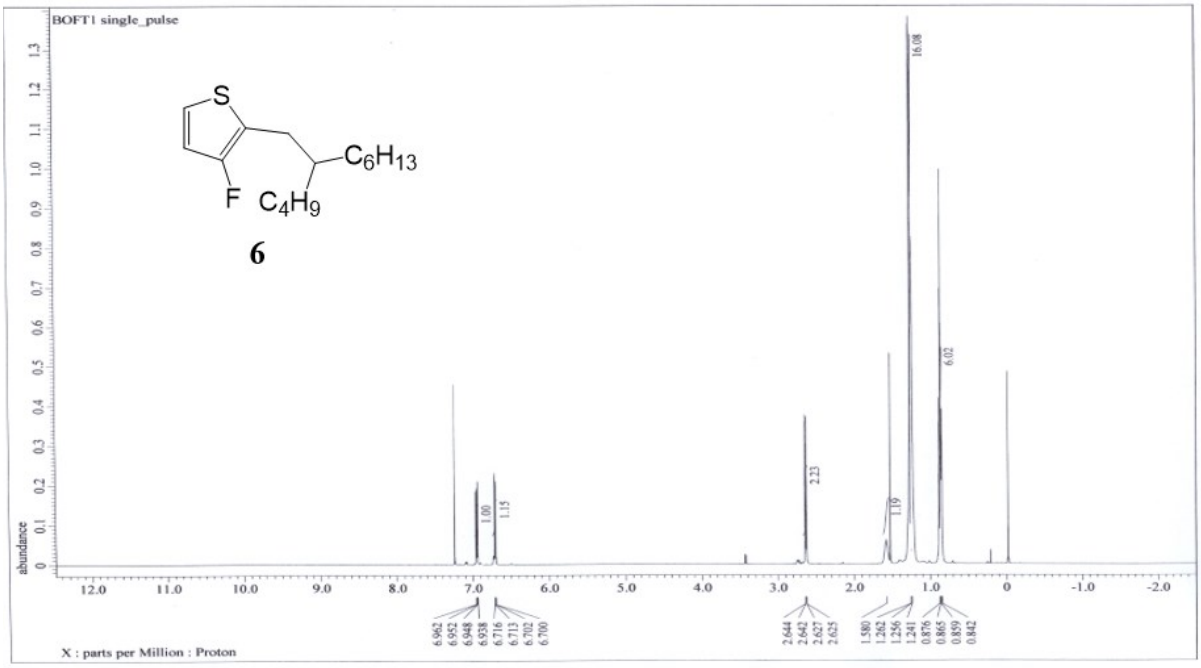

6

BOFT1 single_pulse
S
F
C_6H_{13}
C_4H_9
abundance
0
0.1
0.2
0.3
0.4
0.5
0.6
0.7
0.8
0.9
1.0
1.1
1.2
1.3
1.00
1.15
2.23
1.19
16.08
6.02
12.0
11.0
10.0
9.0
8.0
7.0
6.0
5.0
4.0
3.0
2.0
1.0
0
-1.0
-2.0
6.962
6.952
6.948
6.938
6.716
6.713
6.702
6.700
2.644
2.642
2.627
2.625
1.580
1.262
1.256
1.241
0.876
0.865
0.859
0.842
X : parts per Million : Proton

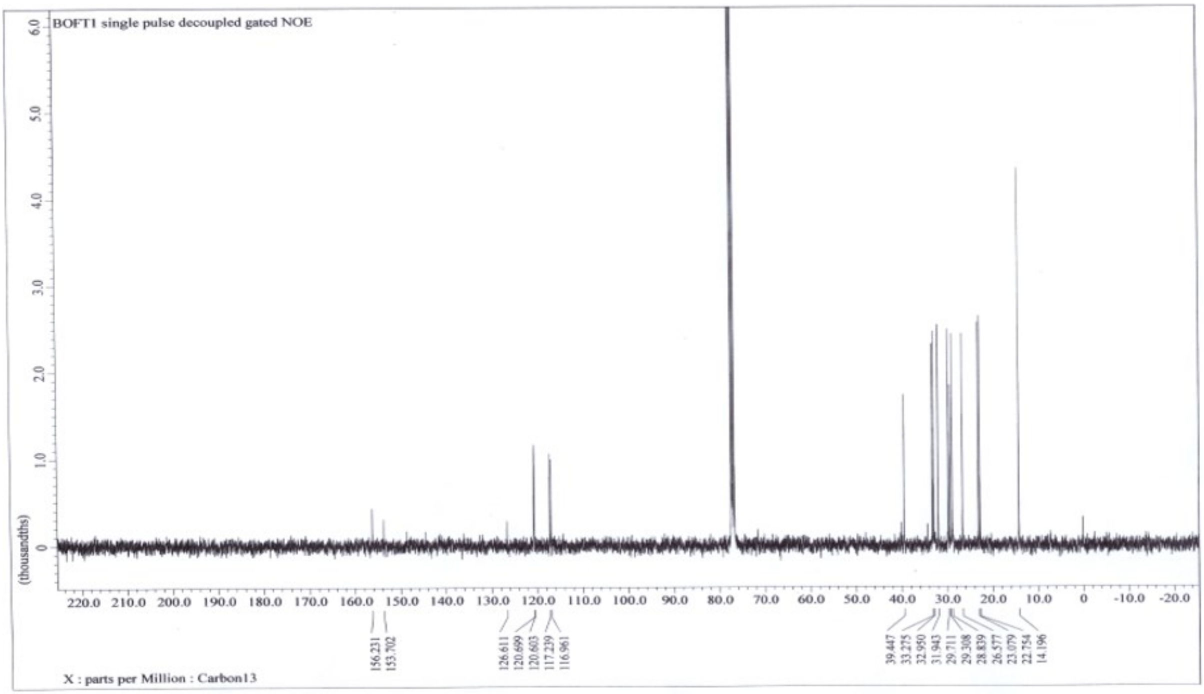

BOFT1 single pulse decoupled gated NOE
(thousandths)
0
1.0
2.0
3.0
4.0
5.0
6.0
220.0
210.0
200.0
190.0
180.0
170.0
160.0
150.0
140.0
130.0
120.0
110.0
100.0
90.0
80.0
70.0
60.0
50.0
40.0
30.0
20.0
10.0
0
-10.0
-20.0
156.231
153.702
126.611
120.699
120.603
117.239
116.961
39.447
33.275
32.950
31.943
29.711
29.308
28.839
26.577
23.079
22.754
14.196
X : parts per Million : Carbon13

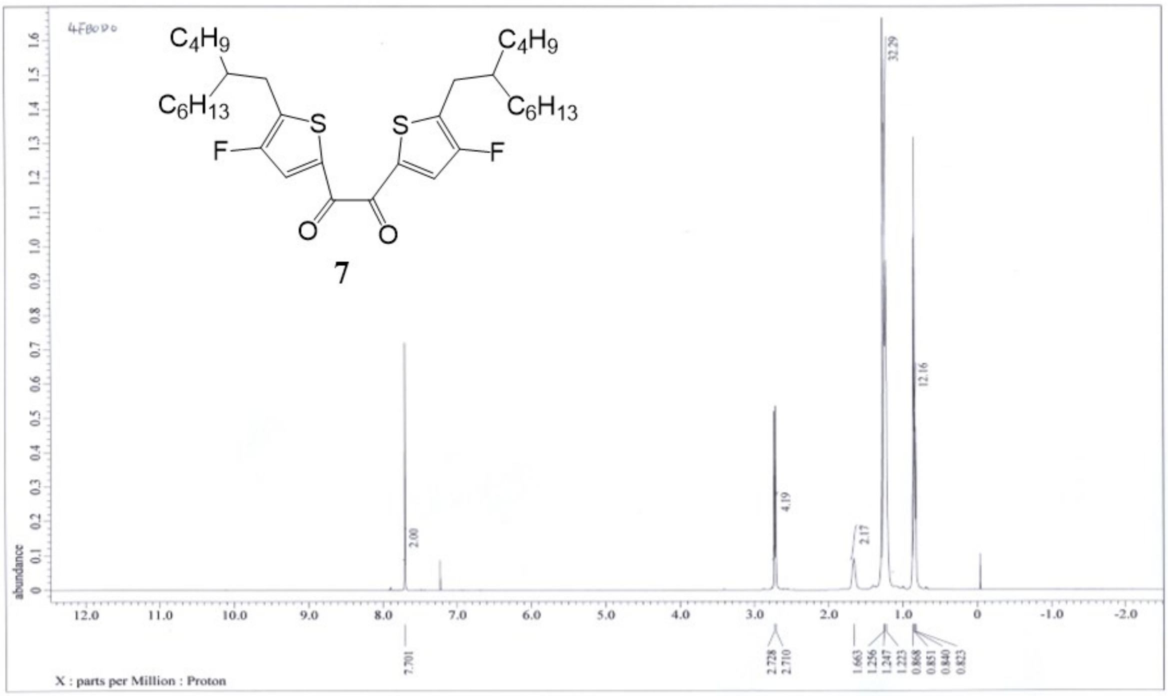
4F80D0
C_4H_9
C_6H_{13}
S
F
O
C_4H_9
C_6H_{13}
S
F
O
7
abundance
1.6
1.5
1.4
1.3
1.2
1.1
1.0
0.9
0.8
0.7
0.6
0.5
0.4
0.3
0.2
0.1
0
2.00
4.19
2.17
32.29
12.16
12.0
11.0
10.0
9.0
8.0
7.0
6.0
5.0
4.0
3.0
2.0
1.0
0
-1.0
-2.0
7.701
2.728
2.710
1.663
1.256
1.247
1.223
0.868
0.851
0.840
0.823
X : parts per Million : Proton

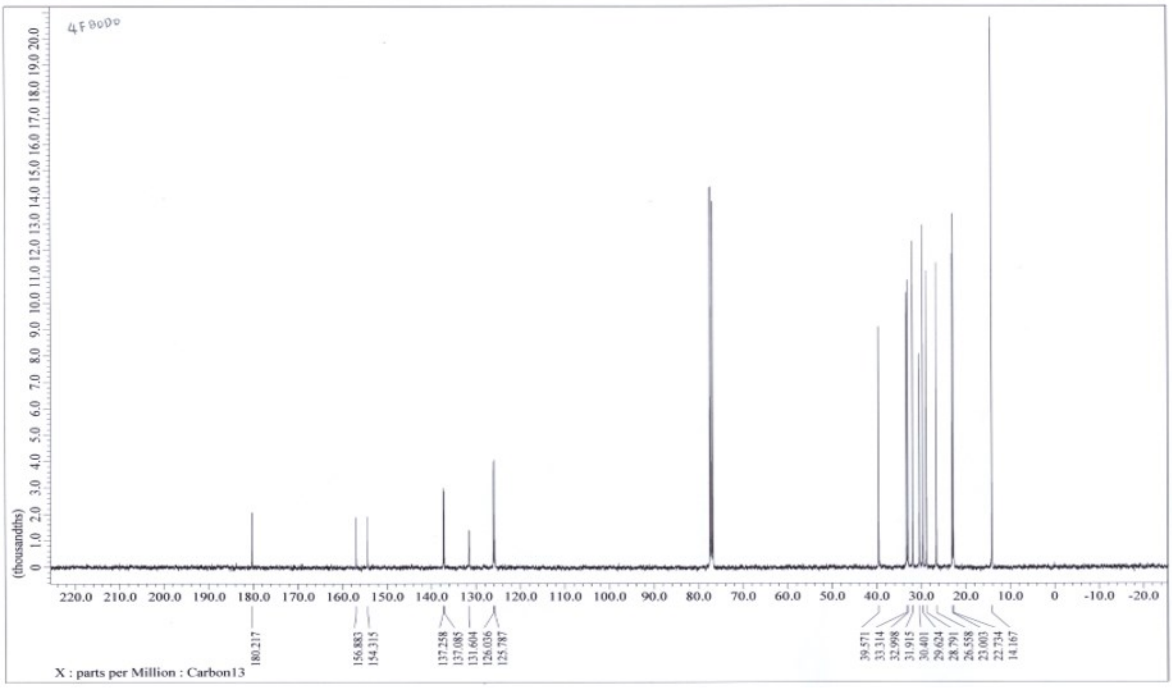
4F80D0
(thousandths)
20.0
19.0
18.0
17.0
16.0
15.0
14.0
13.0
12.0
11.0
10.0
9.0
8.0
7.0
6.0
5.0
4.0
3.0
2.0
1.0
0
220.0
210.0
200.0
190.0
180.0
170.0
160.0
150.0
140.0
130.0
120.0
110.0
100.0
90.0
80.0
70.0
60.0
50.0
40.0
30.0
20.0
10.0
0
-10.0
-20.0
180.217
156.883
154.315
137.258
137.085
131.604
126.036
125.787
39.571
33.314
32.998
31.915
30.401
29.624
28.791
26.558
23.003
22.734
14.167
X : parts per Million : Carbon13

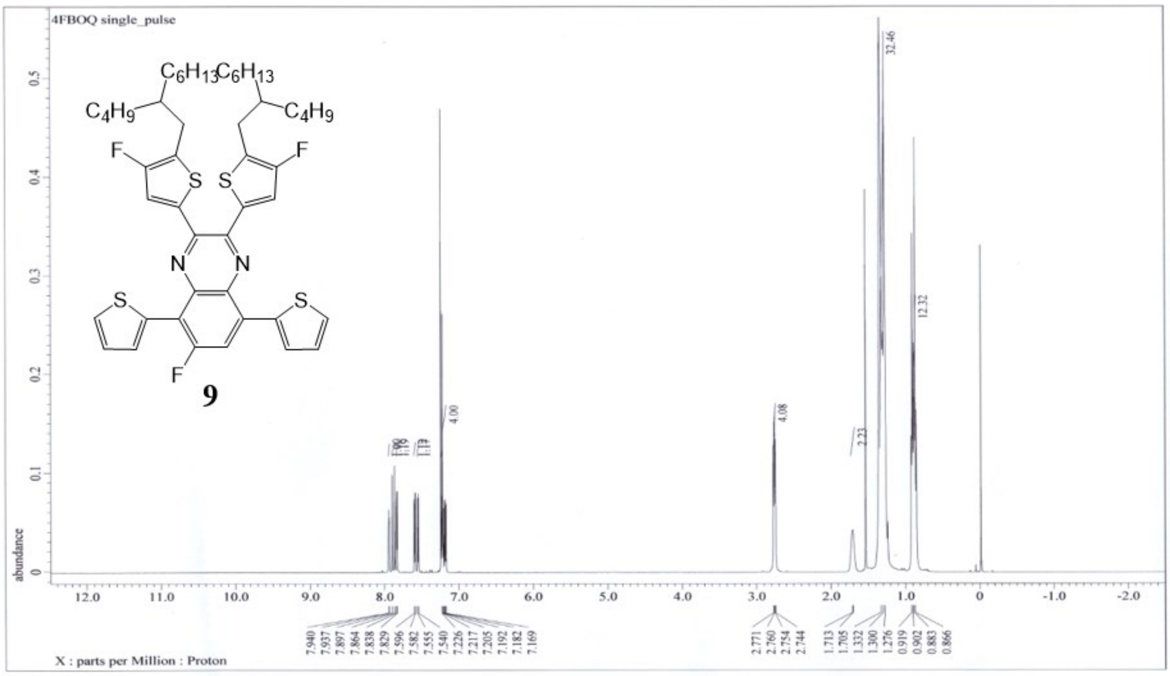
4FBOQ single_pulse
C_6H_{13}
C_6H_{13}
C_4H_9
C_4H_9
F
S
S
F
N
N
S
S
F
9
abundance
0
0.1
0.2
0.3
0.4
0.5
12.0
11.0
10.0
9.0
8.0
7.0
6.0
5.0
4.0
3.0
2.0
1.0
0
-1.0
-2.0
32.46
12.32
4.00
4.08
2.23
7.940
7.937
7.897
7.864
7.838
7.829
7.596
7.582
7.555
7.540
7.226
7.217
7.205
7.192
7.182
7.169
2.771
2.760
2.754
2.744
1.713
1.705
1.332
1.300
1.276
0.919
0.902
0.883
0.866
X : parts per Million : Proton

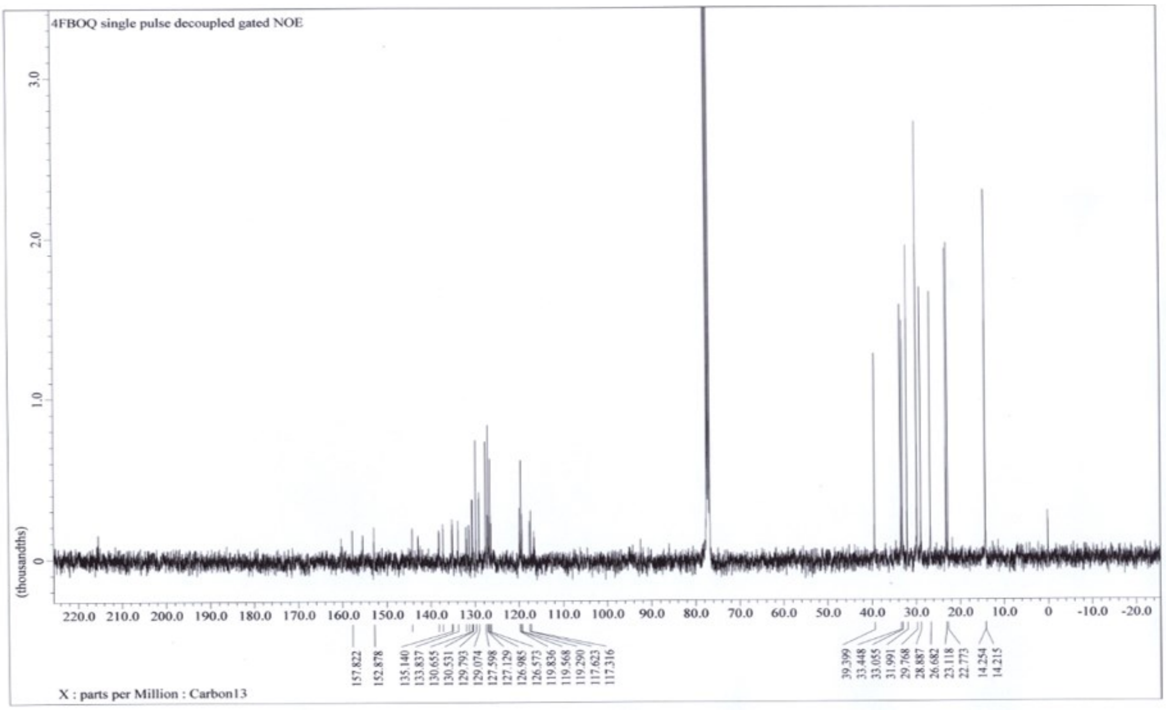
4FBOQ single pulse decoupled gated NOE
(thousandths)
0
1.0
2.0
3.0
220.0
210.0
200.0
190.0
180.0
170.0
160.0
150.0
140.0
130.0
120.0
110.0
100.0
90.0
80.0
70.0
60.0
50.0
40.0
30.0
20.0
10.0
0
-10.0
-20.0
157.822
152.878
135.140
133.837
130.655
130.531
129.793
129.074
127.598
127.129
126.985
126.573
119.836
119.568
119.290
117.623
117.316
39.399
33.448
33.055
31.991
29.768
28.887
26.682
23.118
22.773
14.254
14.215
X : parts per Million : Carbon13

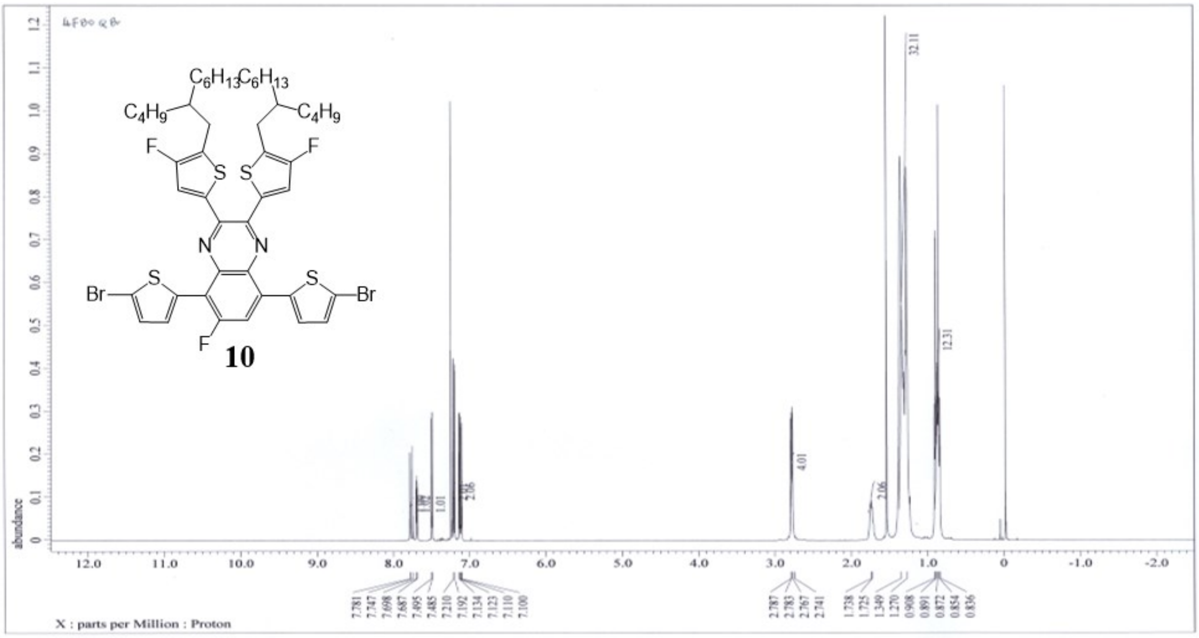
4FBoQBr
C6H13 C6H13
C4H9 C4H9
F F
S S
N N
Br S S Br
F
10
abundance
0 0.1 0.2 0.3 0.4 0.5 0.6 0.7 0.8 0.9 1.0 1.1 1.2
1.01
2.06
4.01
2.06
32.11
12.31
12.0 11.0 10.0 9.0 8.0 7.0 6.0 5.0 4.0 3.0 2.0 1.0 0 -1.0 -2.0
7.781 7.747 7.698 7.687 7.495 7.485 7.210 7.192 7.134 7.123 7.110 7.100
2.787 2.783 2.767 2.741
1.738 1.725 1.349 1.270 0.908 0.891 0.872 0.854 0.836
X : parts per Million : Proton

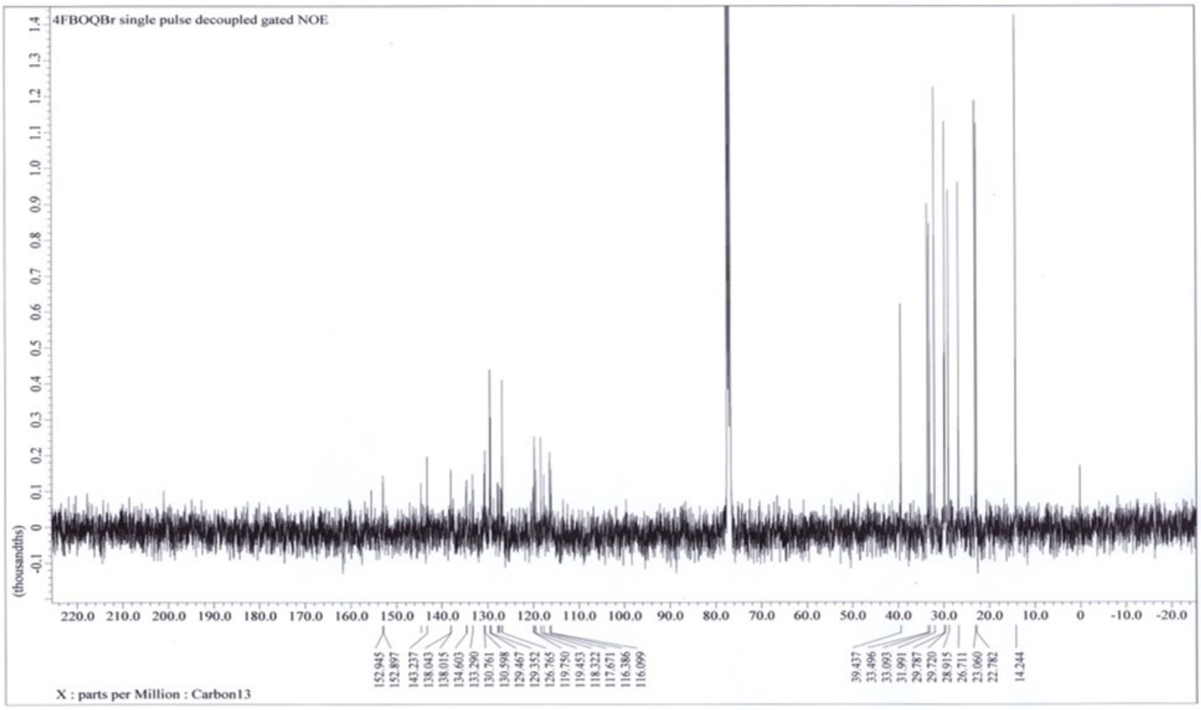
4FBOQBr single pulse decoupled gated NOE
(thousandths)
-0.1 0 0.1 0.2 0.3 0.4 0.5 0.6 0.7 0.8 0.9 1.0 1.1 1.2 1.3 1.4
220.0 210.0 200.0 190.0 180.0 170.0 160.0 150.0 140.0 130.0 120.0 110.0 100.0 90.0 80.0 70.0 60.0 50.0 40.0 30.0 20.0 10.0 0 -10.0 -20.0
152.945 152.897 143.237 138.043 138.015 134.603 133.290 130.761 130.598 129.467 129.352 126.765 119.750 119.453 118.322 117.671 116.386 116.099
39.437 33.496 33.093 31.991 29.787 29.720 28.915 26.711 23.060 22.782
14.244
X : parts per Million : Carbon13

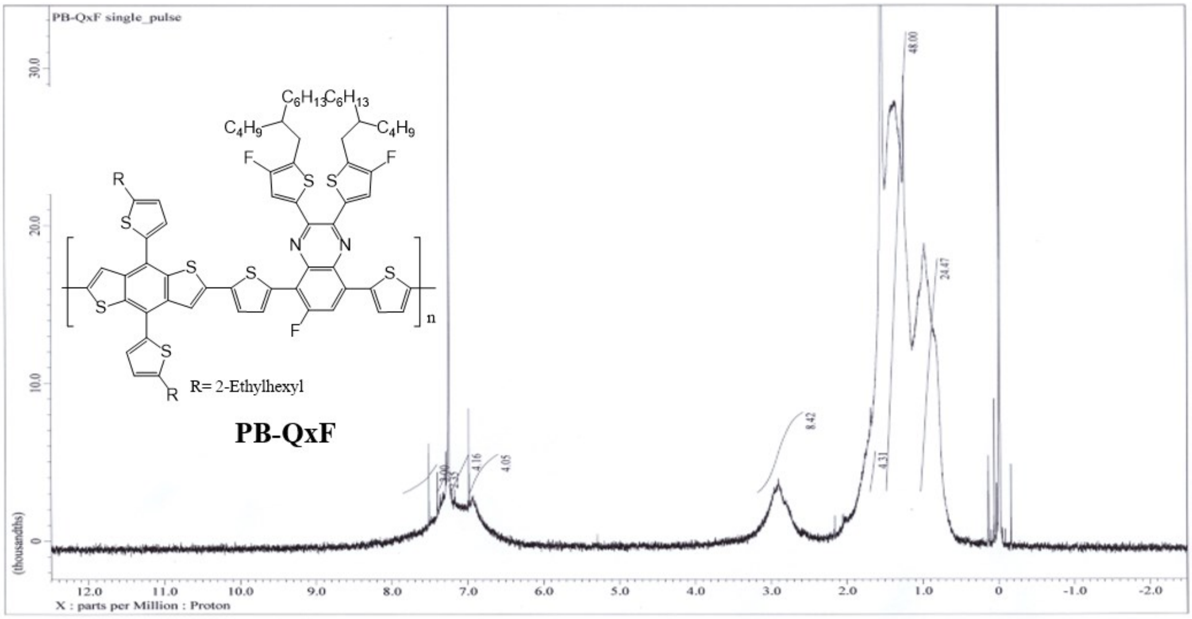
PB-QxF single_pulse
30.0
20.0
10.0
0
(thousandths)
12.0
11.0
10.0
9.0
8.0
7.0
6.0
5.0
4.0
3.0
2.0
1.0
0
-1.0
-2.0
X : parts per Million : Proton
3.00
4.16
4.05
8.42
4.31
48.00
24.47
C_6H_{13}
C_6H_{13}
C_4H_9
C_4H_9
F
F
F
S
N
n
R
R= 2-Ethylhexyl
PB-QxF

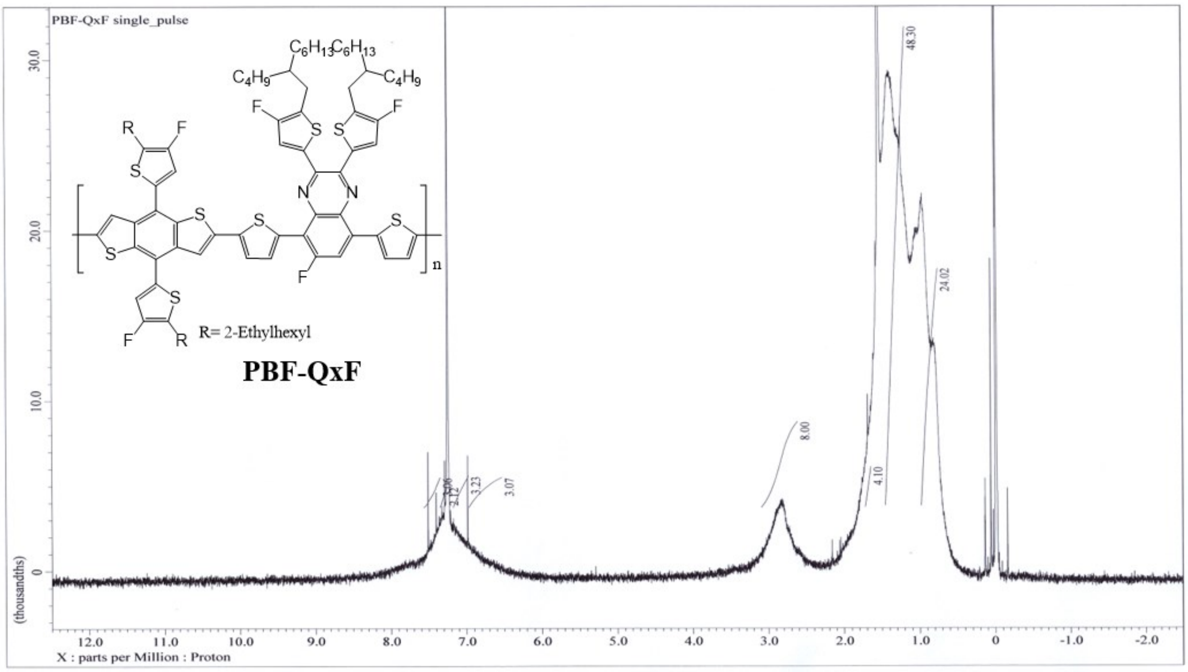
PBF-QxF single_pulse
30.0
20.0
10.0
0
(thousandths)
12.0
11.0
10.0
9.0
8.0
7.0
6.0
5.0
4.0
3.0
2.0
1.0
0
-1.0
-2.0
X : parts per Million : Proton
2.12
3.23
3.07
8.00
4.10
48.30
24.02
C_6H_{13}
C_6H_{13}
C_4H_9
C_4H_9
F
F
F
S
N
n
R
R= 2-Ethylhexyl
PBF-QxF